

Methods

Animals

Male C57BL/6 mice were housed in standard laboratory cages (four to five mice per cage) on a 12-h light/dark cycle (lights on at 8:00 A.M.) in a temperature-controlled room (21-25°C). Mice were 6-8 weeks old at the time of viral infusion. Food and water were given ad libitum. Behavioral testing was performed during the light cycle between 10:00 A.M. and 5:00 P.M. Procedures were conducted in accordance with the Chinese Council on Animal Care Guidelines. Efforts were made to minimize animal suffering and to reduce the number of animals used.

Virus construction and packaging

The recombinant adeno-associated viral vector serotype 2 (AAV2) vectors were serotyped with AAV2 coat proteins and packaged by Sunbio Medical Biotechnology (Shanghai, China). Viral titres are listed below:

AAV2-CaMKII α -hChR2(H134R)-eYFP, 2.8×10^{12} particles/ml

AAV2-CaMKII α -eNpHR3.0-eYFP, 3.0×10^{12} particles/ml

AAV2-CaMKII α -eYFP, 3.0×10^{12} particles/ml

AAV2-DIO-hChR2(H134R)-mCherry, 4.2×10^{12} particles/ml

AAV2-CaMKII α -hM4DGi –mCherry, 3.0×10^{12} particles/ml

AAV2-CaMKII α -mCherry, 3.0×10^{12} particles/ml

The CAV-Cre (5.2×10^{12} particles/ml) vectors were packaged by VTABrain (Wuhan, China).

Virus injection and optical fibre/guide cannula placement

All surgeries were performed under aseptic conditions under stereotaxic guidance. Mice were anaesthetized using 1% pentobarbital sodium and placed into a stereotaxic instrument (RWD, China). All coordinates are relative to bregma in mm³.

Surgery was performed for viral transfection of IL cell somata (coordinates from bregma: +1.75 mm anteroposterior (AP), ± 0.3 mm mediolateral (ML); and – 2.8 mm dorsoventral (DV))(1). Virus (0.3 μ l per side) was injected using a 5- μ l Hamilton syringe with infusion cannulas and a microinjector pump (KDS, Stoelting, USA) at a rate of 0.05 μ l/min. After completion of the injection, the needle was raised 0.1 mm for an additional 10 min to allow diffusion of virus at the injection site and then slowly withdrawn. ChR2 mice received unilateral viral infusion, optical fibre or guide cannula implantation, whereas all eNpHR or hM4DGi mice were bilaterally injected and implanted since unilateral loss-of-function may be compensated by the other hemisphere. All unilateral manipulations, including drug injection, viral injection, and optical fibre or cannula implantation, were counterbalanced across hemispheres.

For experiments stimulating CeM- or Cel-projecting IL neurons, CAV-Cre was injected in the CeM (-1.0 mm AP; ± 2.4 mm ML; -4.6 mm DV) or CeL (-1.4 mm AP; ± 2.9 mm ML; -4.8 mm DV)(2), along with 0.3 μ l of AAV2-DIO-hChR2(H134R)-mCherry injected in the IL (+1.75 mm AP; ± 0.3 mm ML; -2.8 mm DV) at 0.1 μ l/min in the ipsilateral hemisphere.

For optogenetic manipulations of IL somata, an implantable fibre (200- μ m diameter, NA 0.22, Inper, Hangzhou, China) was implanted along the same track over the IL at a depth of -2.4 mm. Behavioral and electrophysiological experiments were conducted with a window of 3-4 weeks (for cell body manipulations) or 8-10 weeks (for all terminal manipulations) after injection to allow for opsin expression.

For optogenetic stimulations of IL terminals in the LS, CeA, BLA, or BNST, optical fibres were placed above the LS (+0.5 mm AP; ± 0.59 mm ML; -2.4 mm DV)(3), CeA-blue light stimulus (15° angle, -2.16 mm AP; ± 2.25 mm ML; -3.98 mm DV), CeA-yellow light stimulus (-1.06 mm AP; ± 2.25 mm ML; -4.4 mm DV)(4), BLA (-1.6 mm AP; ± 3.1 mm ML; -4.5 mm DV)(4), and BNST (+0.2 mm AP; ± 1.0 mm ML; -3.9 mm DV)(5), respectively.

For mice used in drug injection experiments, a small craniotomy was performed, and stainless-steel guide cannulas (62003, RWD, China, length 4.6 mm for CeA, length 2.6 mm for LS) were lowered into the CeA (-1.06 mm AP; ± 2.25 mm ML; -4.4 mm DV) or LS (+0.5 mm AP; ± 0.59 mm ML; -2.4 mm DV). The guide cannulas were secured in place using glass ionomer cements. Dummy cannulas (62102, RWD, China, with lengths matching the guide cannulas) were placed inside the guide cannulas to prevent occlusion. Incisions were fixed and covered with glass ionomer cement. The animals were removed from the stereotaxic instrument and recovered on an electric blanket, and then they were placed back into their home cages. Drugs and optical fibres were delivered through the same guide cannula.

Retrograde labelling

Regarding the red fluorescent retrobeads (Lumafluor), we applied 0.15 μ l directly into the CeA (-1.06 mm AP; ± 2.25 mm ML; -4.7 mm DV) or the LS (+0.5 mm AP; ± 0.59 mm ML; -2.8 mm DV) at 0.05 μ l/min.

For CAV tracing experiments, 0.5 μ l of CAV-Cre was injected in the CeA (-1.06 mm AP; ± 2.25 mm ML; -4.7 mm DV) or the LS (+0.5 mm AP; ± 0.59 mm ML; -2.8 mm DV) at 0.1 μ l/min along with 0.3 μ l of AAV2-DIO-hChR2(H134R)-mCherry injected in the IL (+1.75 mm AP; ± 0.3 mm ML; -2.8 mm DV) at 0.1 μ l/min in the ipsilateral hemisphere.

For CTB tracing experiments, 0.1 μ l of cholera toxin β subunit conjugated to fluorophores (CTB488, C22841; CTB555, C34776, Life Technologies Corporation) was injected unilaterally into the LS (+0.5 mm AP; ± 0.59 mm ML; -2.8 mm DV), and CeA (-1.06 mm AP; ± 2.25 mm ML; -4.7 mm DV) at 0.05 μ l/min in the ipsilateral hemisphere.

Mice were sacrificed 2 weeks after retrobead infusion or 4 weeks after CAV or CTB injection. Brain slices were then obtained as described below in “Histology”.

Electrophysiological recordings

For slice physiology in combination with optogenetics, 4- to 5-week-old C57BL/6 mice were injected with AAV2-CaMKII α -ChR2 (H134R)-eYFP or AAV2-CaMKII α -eNpHR3.0-eYFP into the IL. After a month, acute 300- μ m coronal slices were prepared using a Vibroslice (Leica VT 1000S) in an ice-cold solution that contained 220 mM sucrose, 2.5 mM KCl, 1.3 mM CaCl₂, 2.5 mM MgSO₄, 1 mM NaH₂PO₄, 26 mM NaHCO₃, and 10 mM glucose. Slices were allowed to recover for at least 1.5 h (0.5 h at 34°C followed by 1 h at 25°C) in an ACSF solution containing 126 mM NaCl, 26 mM NaHCO₃, 3.0 mM KCl, 1.2 mM NaH₂PO₄, 2.0 mM CaCl₂, 1.0 mM MgSO₄, and 10 mM glucose. All chemicals were from Sigma-Aldrich. Slices were placed in the recording chamber and superfused (1.5 ml/min) with ACSF at 32-34°C. All solutions were saturated with 95% O₂/5% CO₂. Neurons were visualized with an upright microscope (DM-LFSA; Leica) equipped with both DIC optics and a filter set for visualizing eYFP using a 40x water-immersion objective and a charge-coupled device (CCD) camera (Zeiss, Axioskop2 Fspplus). Action potentials were recorded using whole-cell current-clamp techniques (MultiClamp 700B Amplifier, Digidata 1320A analogue-to-

digital converter) and pClamp 9.2 software (Axon Instruments). Slices containing the IL were used to verify the expression of ChR2 or eNpHR in the IL, and only slices from mice with ChR2 or eNpHR expression restricted to the IL were used. Whole-cell recordings were made from IL neurons using patch electrodes (3-6 M Ω) filled with 105 mM K-gluconate, 30 mM KCl, 10 mM HEPES, 10 mM phosphocreatine, 4 mM ATP-Mg, 0.3 mM GTP-Na, 0.3 mM EGTA, and 5 mM QX314 (pH 7.35, 285 mOsm). Series resistances were typically 10-20 M Ω .

Regarding light delivery, light was emitted from a 300 W broad-wavelength xenon lamp source (DG-4, Sutter Instruments, Novato, CA, USA), bandpass filtered at 470 ± 20 nm (Semrock; Rochester, NY, USA) for blue light stimulation or 590 ± 20 nm (Semrock; Rochester, NY, USA) for yellow light stimulation, passed through additional neutral density filters (ThorLabs; Newton, NJ, USA) and coupled to the fluorescence port of the microscope. Light (5-10 mW/mm²) was delivered to slices through 40x, 0.8 NA objectives. Pulsed input signals were generated from pClamp and delivered to DG-4 via BNC.

To test the monosynaptic response of ChR2 terminal activation, ChR2 was activated using a DG-4 light source, and the sodium channel blocker tetrodotoxin (TTX, 1 μ M) was perfused in combination with the potassium channel blocker 4-aminopyridine (4-AP, 100 μ M) applied to facilitate release from synaptic terminals. The NMDA receptor antagonist AP5 (50 μ M) and AMPA receptor antagonist NBQX (20 μ M) were applied to block glutamate receptors.

For chemogenetic treatment, CNO (5 μ M) was bath applied, and changes in membrane potential were monitored.

Light delivery

For optical stimulation during behavioral assays, the laser was first connected to a patch cord with a pair of FC/PC connectors at each end (Thorlabs, Newton, NJ). This patch cord was connected through a fibre-optic rotary joint (Thorlabs, Newton, NJ), which allows free rotation of the fibre, with another patch cord with a side of FC/PC connector and a side that delivers the laser via either chronic optic fibres or a guide cannula. For all eNpHR mice, 10 mW of constant yellow light generated by a 100-mW, 594-nm DPSS laser (Thinker Tech Nanjing Biotech Co. Ltd., China). Blue light was generated by a 100-mW, 473-nm DPSS laser (Thinker Tech Nanjing Biotech Co. Ltd., China), while light output was controlled using a pulse generator (Thinker Tech Nanjing Biotech Co. Ltd., China) to deliver 5-ms light pulse trains at 20 Hz. Light stimulation protocols were specified by group. ChR2-expressing IL neurons were directly illuminated at 3 mW, and higher light power induced seizures(6). To manipulate the activity of IL terminals in the CeA, BLA, BNST and LS, 7-8 mW, 3-5 mW, 10-15 mW and 10-15 mW light power, respectively, were used as previously reported(3-5).

Drug delivery

For glutamate receptor antagonist infusion, the solution consisted of 10 mM 2,3-dihydroxy-6-nitro-7-sulfamoyl-benzo[f]quinoxaline-2,3-dione (NBQX; Tocris, Ellisville MO, USA) and 50 mM d(-)-2-amino-5-phosphonopentanoic-acid (AP5; Sigma-Aldrich, USA) dissolved in ACSF(7). For all hM4DGi mice, 5 μ M clozapine-N-oxide (CNO, Sigma, USA) was used. Thirty minutes before the behavioral assays, 0.3 μ l of solution was infused via infusion cannulas at a flow rate of 0.1 μ l/min. The infusion cannulas (62203, RWD, China, length C = 0 mm, G = 0.4 mm) were connected via polyethylene tubing (62302, RWD, China) to 10- μ l microsyringes (Hamilton, Reno, NV) mounted

on a microinfusion pump (RWD200, China). To allow for the diffusion of the drug, the infusion cannulas were kept in place for 5 min before being replaced with dummy cannulas.

Behavioral assays

All mice were handled for three days before behavioral assays for 5 min per day to reduce stress introduced by contact with the experimenter. Five minutes were allowed for recovery in the home cage from handling associated with connecting the optical fibre or cannula before the session was initiated.

The elevated plus maze test (EPM). The elevated plus maze was made of plastic and consisted of two grey open arms (10×50 cm) and two grey enclosed arms ($10 \times 50 \times 40$ cm) extending from a central platform (10×10 cm) at 90 degrees in the form of a plus. Arms of the same type faced each other. The maze was placed 40 cm above the floor. Mice were individually placed in the center, with the head facing a closed arm. For optogenetic experiments, a 9-min EPM session was divided into three 3-min epochs: the prestimulation light-off epoch, the light-on epoch and the poststimulation light-off epoch (off-on-off epochs). For pharmacogenetic experiments, the EPM consisted of a 5-min session.

The open field test (OFT). The open-field chamber (50×50 cm) was made of plastic and was divided into a central field (center, 25×25 cm) and an outer field (periphery). Individual mice were placed in the periphery of the field at the start of the test. For optogenetic experiments, the OFT consisted of a 9-min session in which there were three alternating 3-min epochs (OFF-ON-OFF epochs). For pharmacogenetic experiments, the OFT consisted of a 5-min session.

The EPM and OFT sessions were recorded by a video camera. The EthoVision XT video tracking system (Noldus, Wageningen, Netherlands) was used to track mouse location, velocity, and movement of the head, body, and tail. All measurements displayed are relative to the mouse body.

Fear conditioning and fear extinction procedures. The fear conditioning test was conducted in sound-attenuating chambers on metal grid floors that could generate foot shock (Coulbourn Instruct). Mice were subjected to four fear conditioning pairs of a 30-s conditioned stimulus (CS) (tone at 75 dB, 2800 Hz) and foot shock (1 s, 0.5 mA) at the end of the CS. The internal interval was 1 min. Mouse freezing was monitored by an infrared camera and analysed using Coulbourn-PC software. Fear retrieval, extinction and extinction retrieval were conducted by placing mice in a different chamber, where the metal grid floor was covered and the walls were replaced with white plastic. We applied a continuous auditory tone (180 s, 2800 Hz) during fear retrieval and extinction retrieval sessions on days 2 and 4. The extinction trial was carried out with ten discrete CS presentations (30 s, 2800 Hz) at random intervals (60 s-120 s). For optogenetic experiments (Figure 6, Figure 7), light stimulation accompanied by tone was delivered(8). For a separate fear extinction test (Supplementary figure 9B), mice expressing Chr2 were illuminated for 31 s (1 s before, 30 s during the tone), while mice expressing eNpHR were illustrated for 40 s (10 s before, 30 s during the tone) according to a previous report(9).

Restraint stress. In a room distinct from those used for anxiety-like behavioral testing, the mice were placed in plastic tubes with numerous holes for a period of 1 h. A reversible flapper was placed around the other end of the cylinder to prevent the mouse from backing out of the restraint tube. The mice were then removed from the tubes and transported back to the home cage. The control mice were transported to the room distinct from those used for anxiety-like behavioral testing for 2 h without being subjected to restraint stress, and then, they were moved back to the home cage.

Histology and imaging

Anaesthetized mice were transcardially perfused with ice-cold 4% paraformaldehyde (PFA) in PBS (pH 7.4). Brains were fixed overnight in 4% PFA and then equilibrated in 30% sucrose in PBS. Forty-micrometer-thick coronal slices were cut on a freezing microtome (Leica CM1950) after the brains were sunken in sucrose solution.

We first verified that the virus injections were localized to the target brain regions (IL). Brain regions were determined by anatomical landmarks (such as the forceps minor of the corpus callosum) and were based on the Mouse Brain Atlas in Stereotaxic Coordinates, second edition. Only the mice with the virus expressed strictly in the IL cortex were used.

For the retrograde tracing experiment, we first confirmed that the retrobeads or CTB injections were localized to the target brain regions (LS and CeA). Coronal sections containing the IL were cut, and brain slices from 1.98 to 1.42 mm relative to bregma were used to access the IL. Every 4th slice was selected for analysis of all retrobead- or CTB-labelled cells within the IL, 3 mice per group, and 4 brain slices per mouse.

For immunocytochemistry, sections were washed with PBS three times and were then blocked in 5% normal goat serum solution containing 0.5% Triton X-100 for 2 h at room temperature. Then, slices were incubated with primary antibody (anti-GFP, 1: 1000, G10362, Invitrogen; anti-RFP, 1: 1000, Rockland, 600-401-379; anti-cFos, 1: 500, ABE457, Millipore; anti-PKC δ , 1: 500, #610398, BD Biosciences; anti-SST, 1: 500, MAB354, Millipore) at 4 °C overnight and washed three times in PBS before incubation for 2 h at room temperature with Alexa Fluor-conjugated secondary antibodies (1:500, goat anti-rabbit IgG (H+L) secondary antibody, Alexa Fluor® 488 conjugate, A-11008; goat anti-mouse IgG (H+L) secondary antibody, Alexa Fluor® 647 conjugate, A-32728; goat anti-rat IgG (H+L) secondary antibody, Alexa Fluor 594 conjugate, 11007; Invitrogen).

Images were acquired using a Nikon A1 confocal microscope. All images were taken in roughly the same imaging area and were processed with NIH ImageJ software. Cell counting was performed blinded to the treatment groups.

Statistics

No specific method was used to predetermine the ideal sample size or to randomly assign subjects to the experimental groups. Sample sizes are indicated in Supplementary Table 1 and are similar to those reported in previous studies(8, 10). The normality of the data distribution was confirmed by the Shapiro-Wilk normality test. Statistical differences of normally distributed data were then determined using two-way repeated measures ANOVA, Kruskal-Wallis ANOVA or one-way ANOVA followed by post hoc Bonferroni analysis, Mann-Whitney U test, two-sided or Tukey's multiple comparisons as indicated in Supplemental Table 1. All data were analysed with SPSS software. *P < 0.05, **P < 0.01, ***P < 0.001. See Supplementary Table 1 for statistical details.

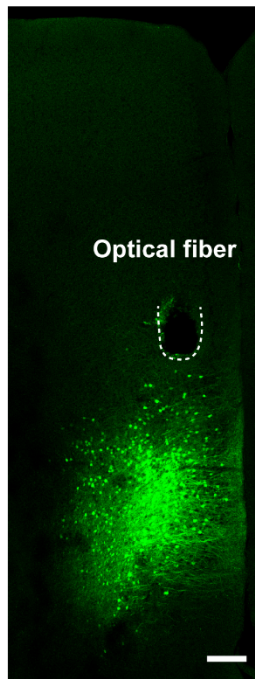
References

1. Bi, L.L., Wang, J., Luo, Z.Y., Chen, S.P., Geng, F., Chen, Y.H., Li, S.J., Yuan, C.H., Lin, S., and Gao, T.M. 2013. Enhanced excitability in the infralimbic cortex produces anxiety-like behaviors. *Neuropharmacology* 72:148-156.
2. Haubensak, W., Kunwar, P.S., Cai, H., Cioocchi, S., Wall, N.R., Ponnusamy, R., Biag, J., Dong,

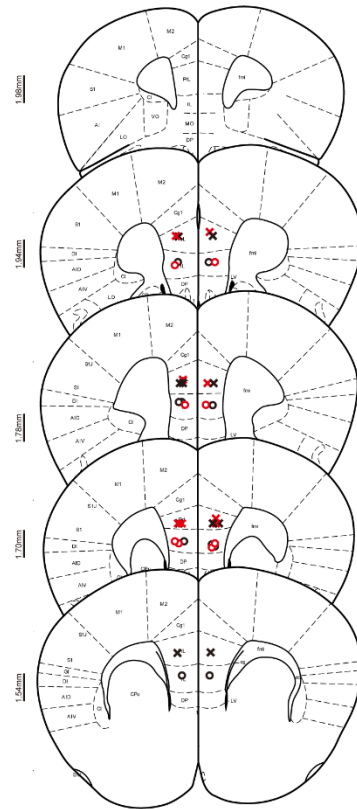
- H.W., Deisseroth, K., Callaway, E.M., et al. 2010. Genetic dissection of an amygdala microcircuit that gates conditioned fear. *Nature* 468:270-276.
3. Anthony, T.E., Dee, N., Bernard, A., Lerchner, W., Heintz, N., and Anderson, D.J. 2014. Control of stress-induced persistent anxiety by an extra-amygdala septohypothalamic circuit. *Cell* 156:522-536.
 4. Tye, K.M., Prakash, R., Kim, S.-Y., Fenno, L.E., Grosenick, L., Zarabi, H., Thompson, K.R., Gradinaru, V., Ramakrishnan, C., and Deisseroth, K. 2011. Amygdala circuitry mediating reversible and bidirectional control of anxiety. *Nature* 471:358-362.
 5. Jennings, J.H., Sparta, D.R., Stamatakis, A.M., Ung, R.L., Pleil, K.E., Kash, T.L., and Stuber, G.D. 2013. Distinct extended amygdala circuits for divergent motivational states. *Nature* 496:224-228.
 6. Warden, M.R., Selimbeyoglu, A., Mirzabekov, J.J., Lo, M., Thompson, K.R., Kim, S.Y., Adhikari, A., Tye, K.M., Frank, L.M., and Deisseroth, K. 2012. A prefrontal cortex-brainstem neuronal projection that controls response to behavioural challenge. *Nature* 492:428-432.
 7. Kim, S.Y., Adhikari, A., Lee, S.Y., Marshel, J.H., Kim, C.K., Mallory, C.S., Lo, M., Pak, S., Mattis, J., Lim, B.K., et al. 2013. Diverging neural pathways assemble a behavioural state from separable features in anxiety. *Nature* 496:219-223.
 8. Adhikari, A., Lerner, T.N., Finkelstein, J., Pak, S., Jennings, J.H., Davidson, T.J., Ferenczi, E., Gunaydin, L.A., Mirzabekov, J.J., Ye, L., et al. 2015. Basomedial amygdala mediates top-down control of anxiety and fear. *Nature* 527:179-185.
 9. Do-Monte, F.H., Manzano-Nieves, G., Quinones-Laracuente, K., Ramos-Medina, L., and Quirk, G.J. 2015. Revisiting the role of infralimbic cortex in fear extinction with optogenetics. *J Neurosci* 35:3607-3615.
 10. Felix-Ortiz, A.C., Beyeler, A., Seo, C., Leppla, C.A., Wildes, C.P., and Tye, K.M. 2013. BLA to vHPC inputs modulate anxiety-related behaviors. *Neuron* 79:658-664.

Supplementary figures

A

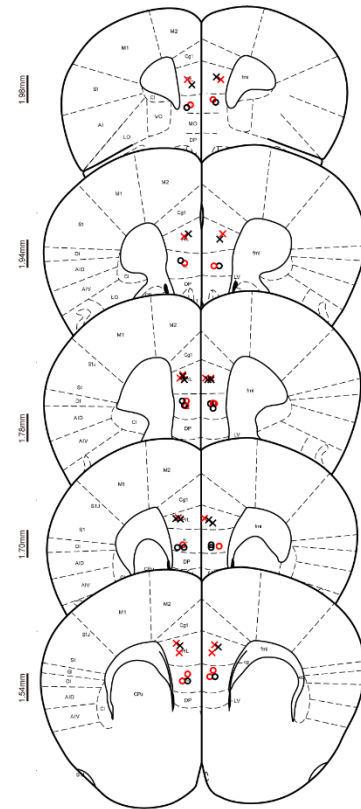


B



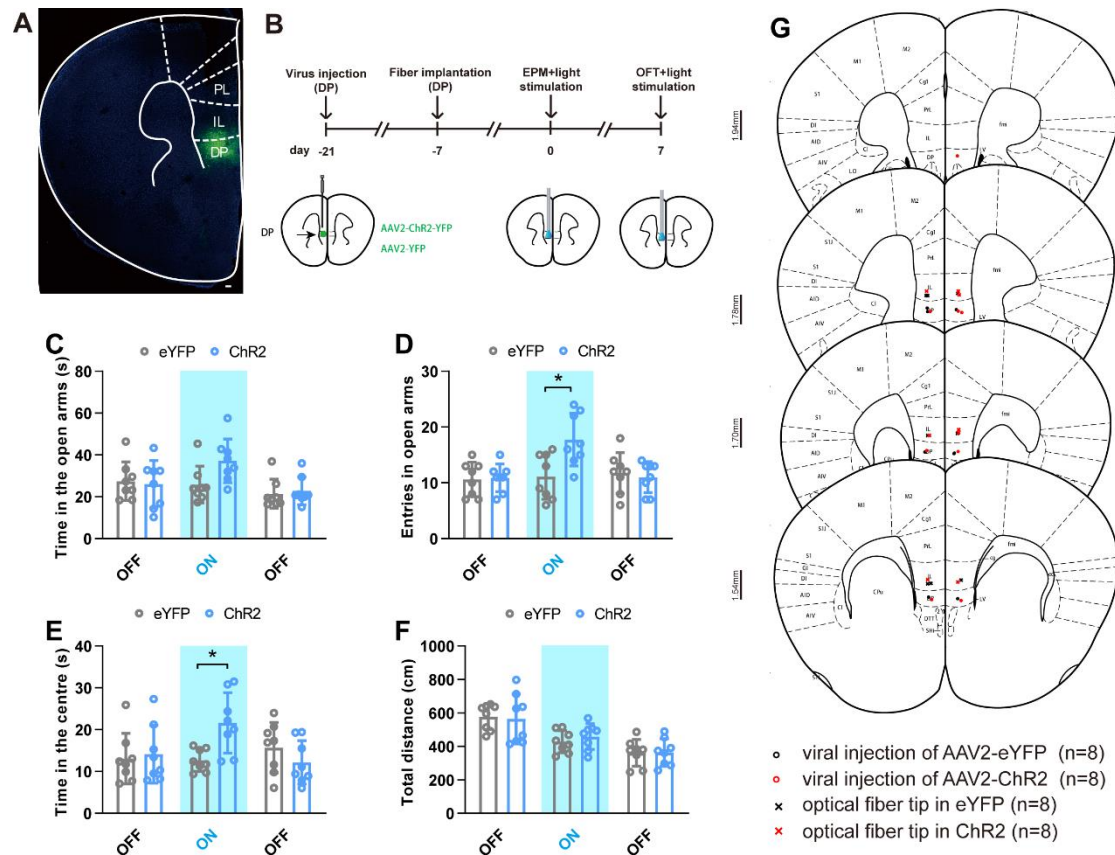
- × viral injection of AAV2-eYFP (n=10)
- × viral injection of AAV2-ChR2 (n=8)
- optical fiber tip in eYFP: IL (n=10)
- optical fiber tip in ChR2: IL (n=8)

C

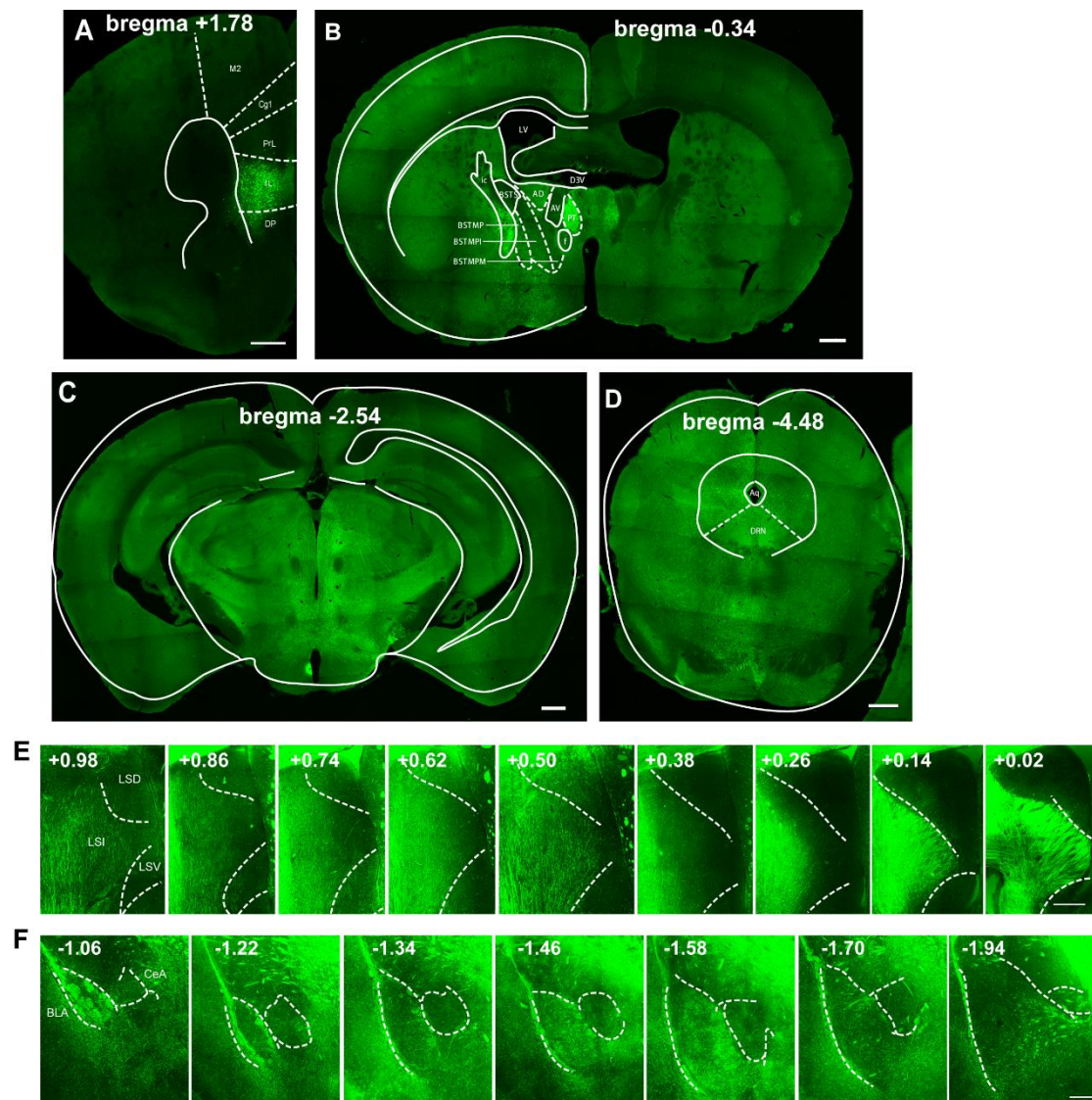


- × viral injection of AAV2-eYFP (n=7)
- × viral injection of AAV2-eNpHR (n=7)
- optical fiber tip in eYFP: IL (n=7)
- optical fiber tip in eNpHR: IL (n=7)

Supplementary Figure 1 Histologically verified placement of viral injections and optic fibres in the ChR2, eNpHR and eYFP groups. Related to Figure 1. Scale bar: 200 μ m.

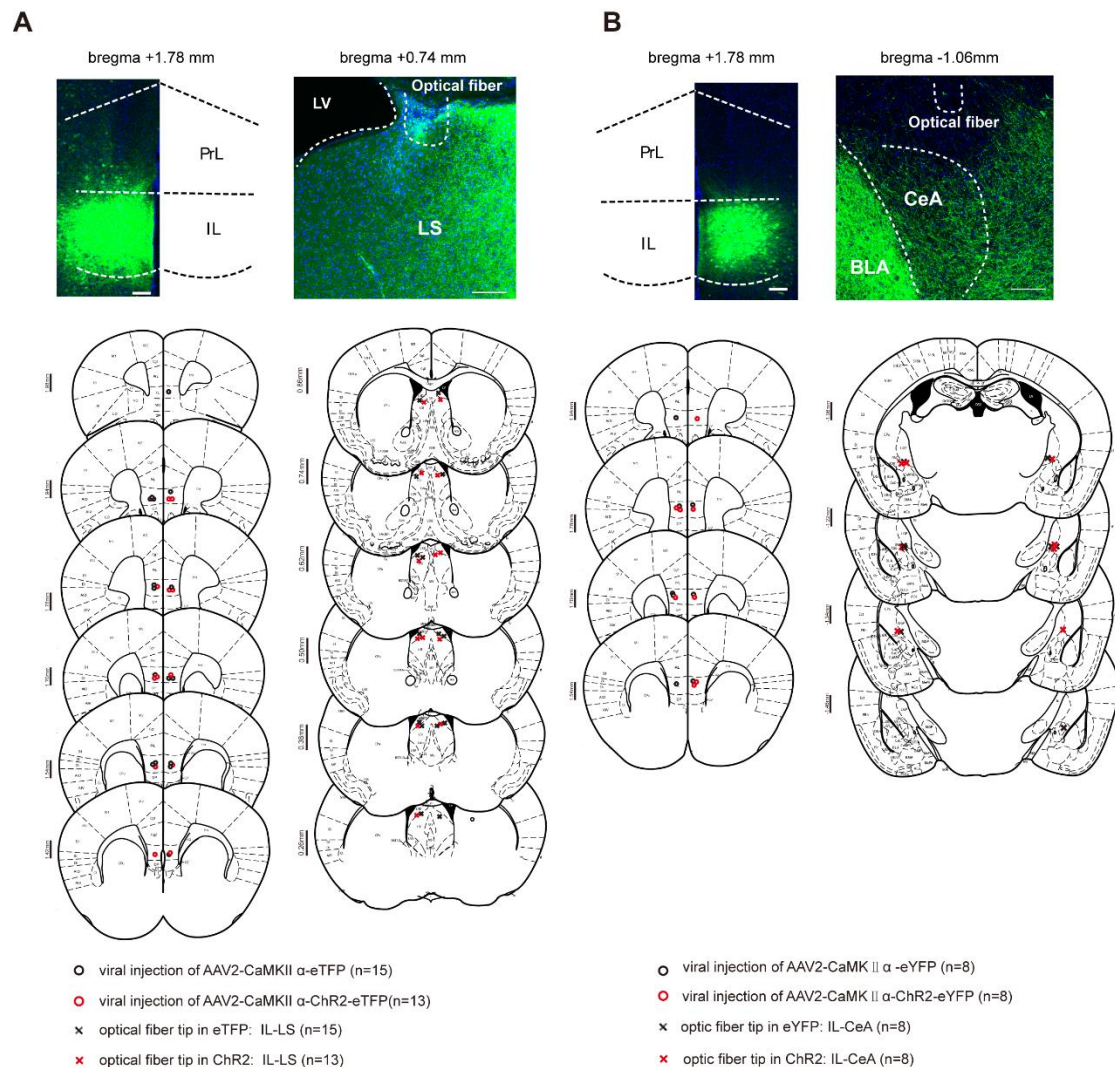


Supplementary Figure 2 Activation of DP with ChR2 decreases anxiety-related behaviours. **A**, Expression of ChR2 in DP; scale bar: 500 μ m. **B**, Schematic of the protocol used for investigating the behavioural impact of optogenetic activation of DP somas. **C**, **D**, ChR2 mice (n = 8 mice) showed a significantly higher probability of entering open arms than eYFP mice (n = 8 mice) during photostimulation (**C**, $F_{\text{Interaction}}(2,28) = 3.183$, $p = 0.0568$; **D**, $F_{\text{Interaction}}(2,28) = 4.989$, $p = 0.0140$). **E**, During the illumination epoch, ChR2 mice spent significantly more time exploring the centre of the open field than eYFP mice ($F_{\text{Interaction}}(2,28) = 5.337$, $p = 0.0109$). **F**, Photostimulation did not alter the distance travelled in either group ($F_{\text{Interaction}}(2,28) = 0.2826$, $p = 0.7785$). **G**, Histologically verified placement of viral injections and optic fibres in the ChR2 and eYFP groups. Statistics in **C-F** reflect two-way repeated-measures ANOVA with Bonferroni post hoc analysis. Data are presented as the mean \pm S.E.M., * $P < 0.05$. See Supplemental Table 1 for statistical details.

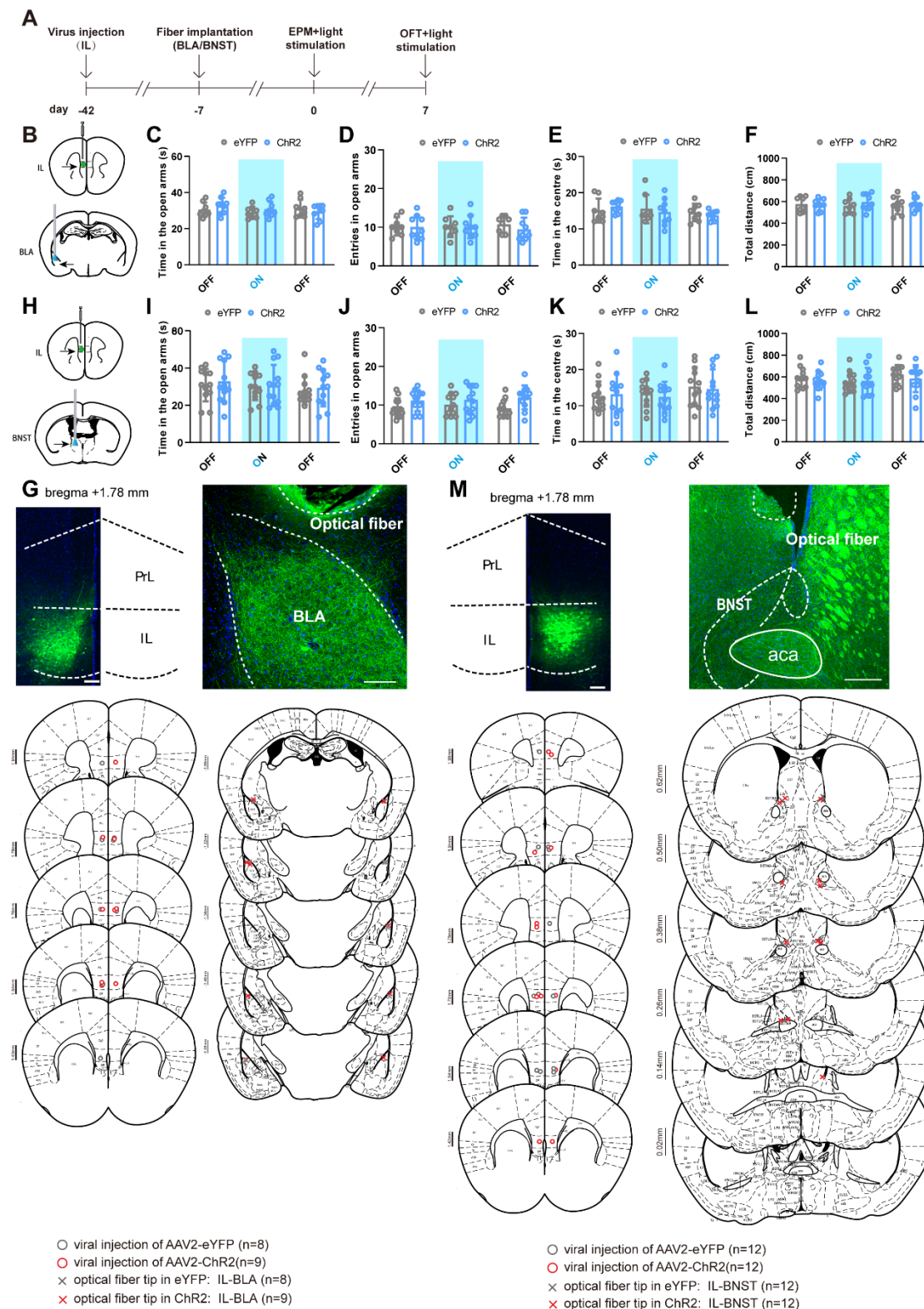


Supplementary Figure 3 Anterograde tracing. **A**, Confocal image of a coronal section containing the IL from a Chr2-eYFP mouse. Scale bar represents 500 μ m. **B-D**, IL glutamatergic neurons innervate the bed nucleus of the stria terminalis (**B**), thalamus (**C**) and dorsal raphe (**D**). **E**, Representative images showing eYFP expression in the LS along the anterior-posterior axis. **F**, Representative images showing eYFP expression in the BLA and CeA along the anterior-posterior axis. Aq: aqueduct; BLA: basolateral amygdala; BSTS: bed nucleus of stria terminalis, supracapsula part; BSTMP: bed nucleus of the stria terminalis, medial division, posterior part; BSTMPL: bed nucleus of the stria terminalis, medial division, posterolateral part; BSTMPM: bed nucleus of the stria terminalis, medial division, posteromedial part; CeA: central amygdala; Cg1: cingulate cortex, area 1; DP: dorsal peduncular cortex; DRN: dorsal raphe nucleus; IL: infralimbic cortex; LSD: the dorsal part of the lateral septum; LSI: intermediate part of

the lateral septum; LSV: ventral part of the lateral septum; M2: secondary motor cortex; PAG: periaqueductal grey; PrL: prelimbic cortex; SC: phoscaid thalamic nucleus. A-D, scale bar represents 500 μm . E-F, scale bar represents 200 μm .

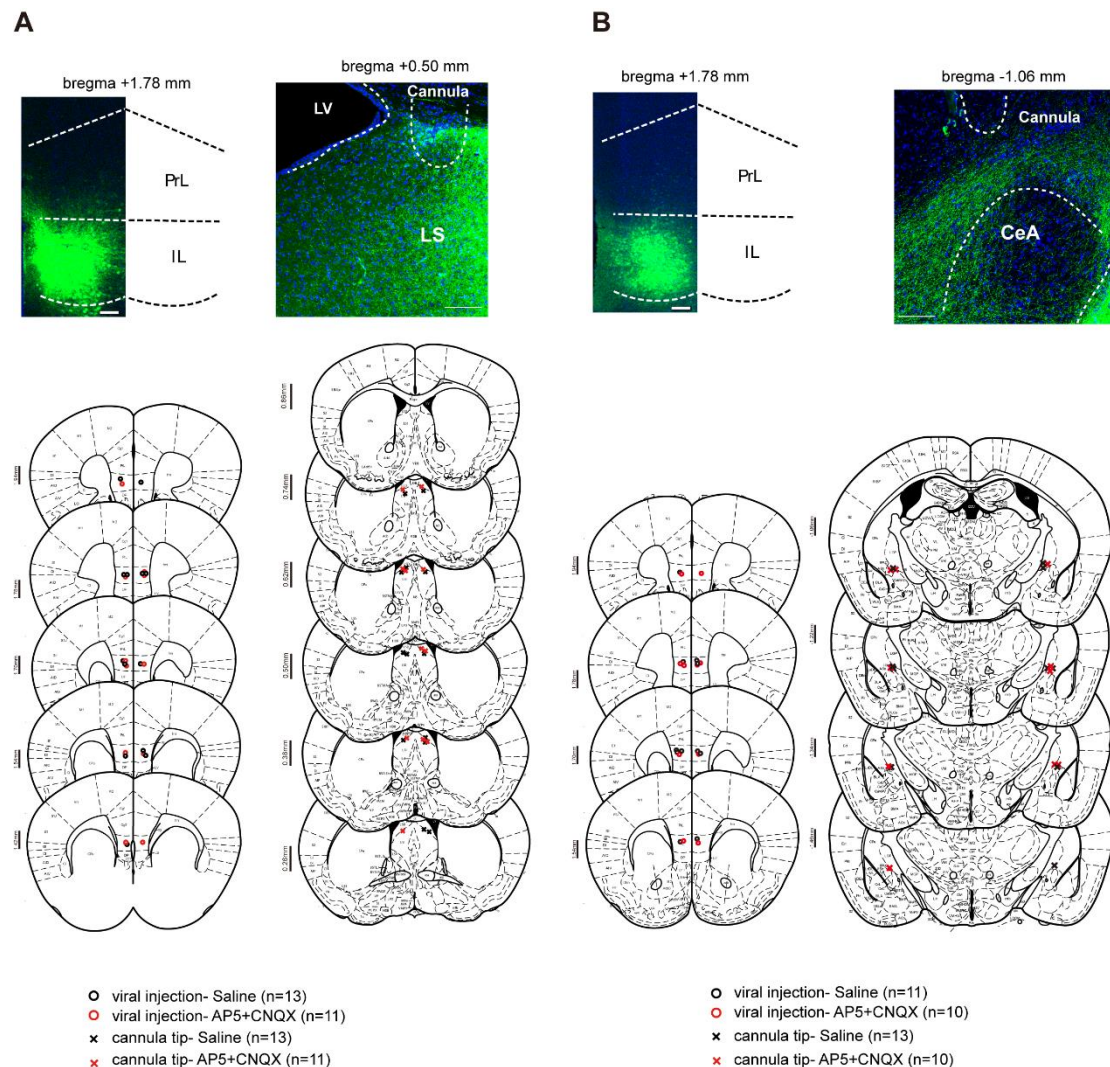


Supplementary Figure 4 Histologically verified placement of viral injections and optic fibres in the ChR2 and eYFP groups. Related to Figure 2. **A**, Left, centre of the viral injection in the IL for all of the animals analysed in Figure 2E-H; right, location of the optic fibre tip above the LS for all of the animals analysed in Figure 2E-H. **B**, Left, centre of the viral injection in the IL for all of the animals analysed in Figure 2J-M; right, location of the optic fibre tip above the CeA for all of the animals analysed in Figure 2J-M. Scale bar represents 100 μ m.

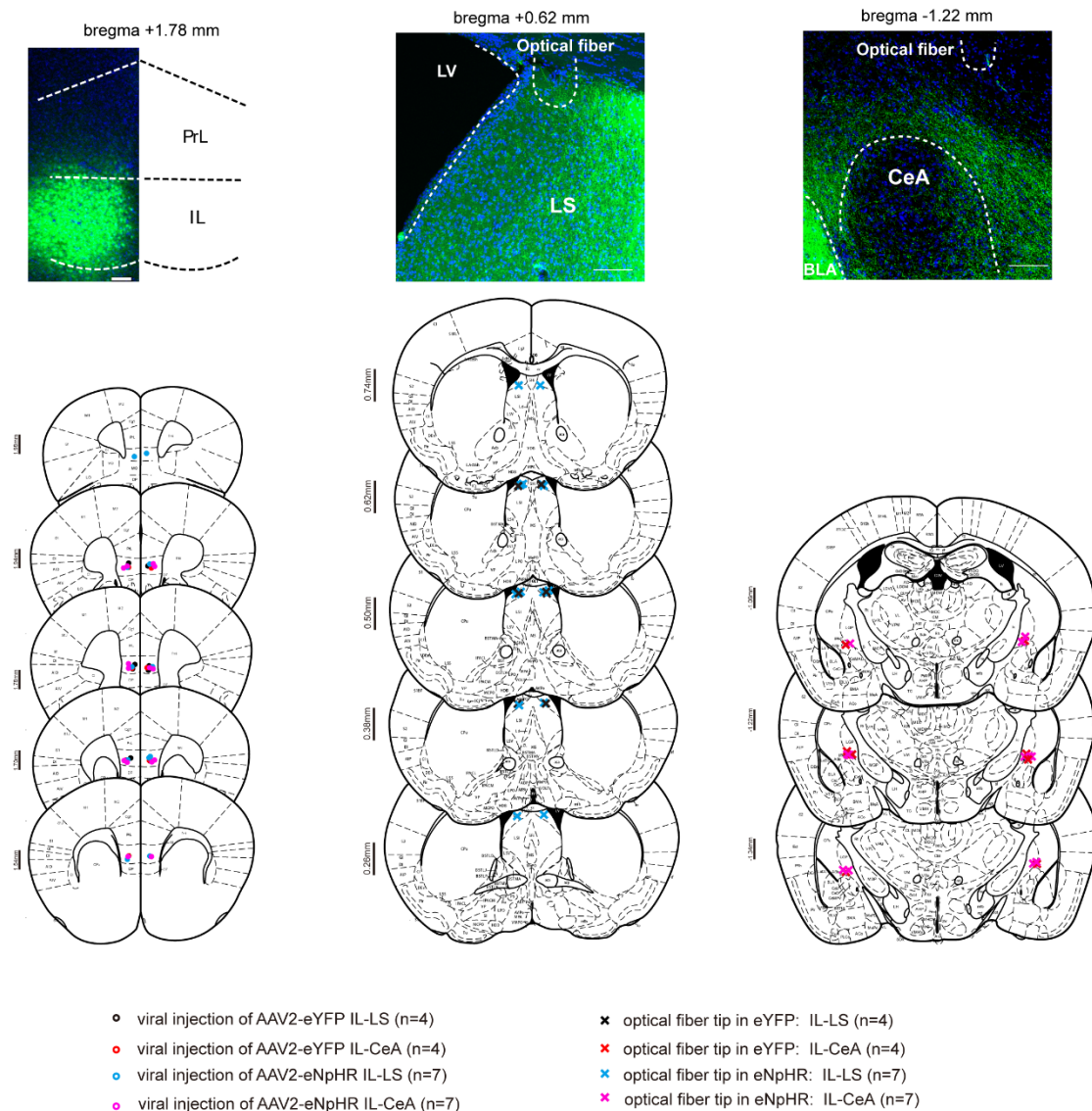


Supplementary Figure 5 Activation of IL-BLA or IL-BNST projections has no effects on anxiety-related behaviours. **A**, Experimental design for investigating the behavioural impact of optogenetic activation of IL-BLA or IL-BNST projections. **B**, eYFP and ChR2 mice expressing eYFP or ChR2-eYFP, respectively, in the IL with optic fibres above the

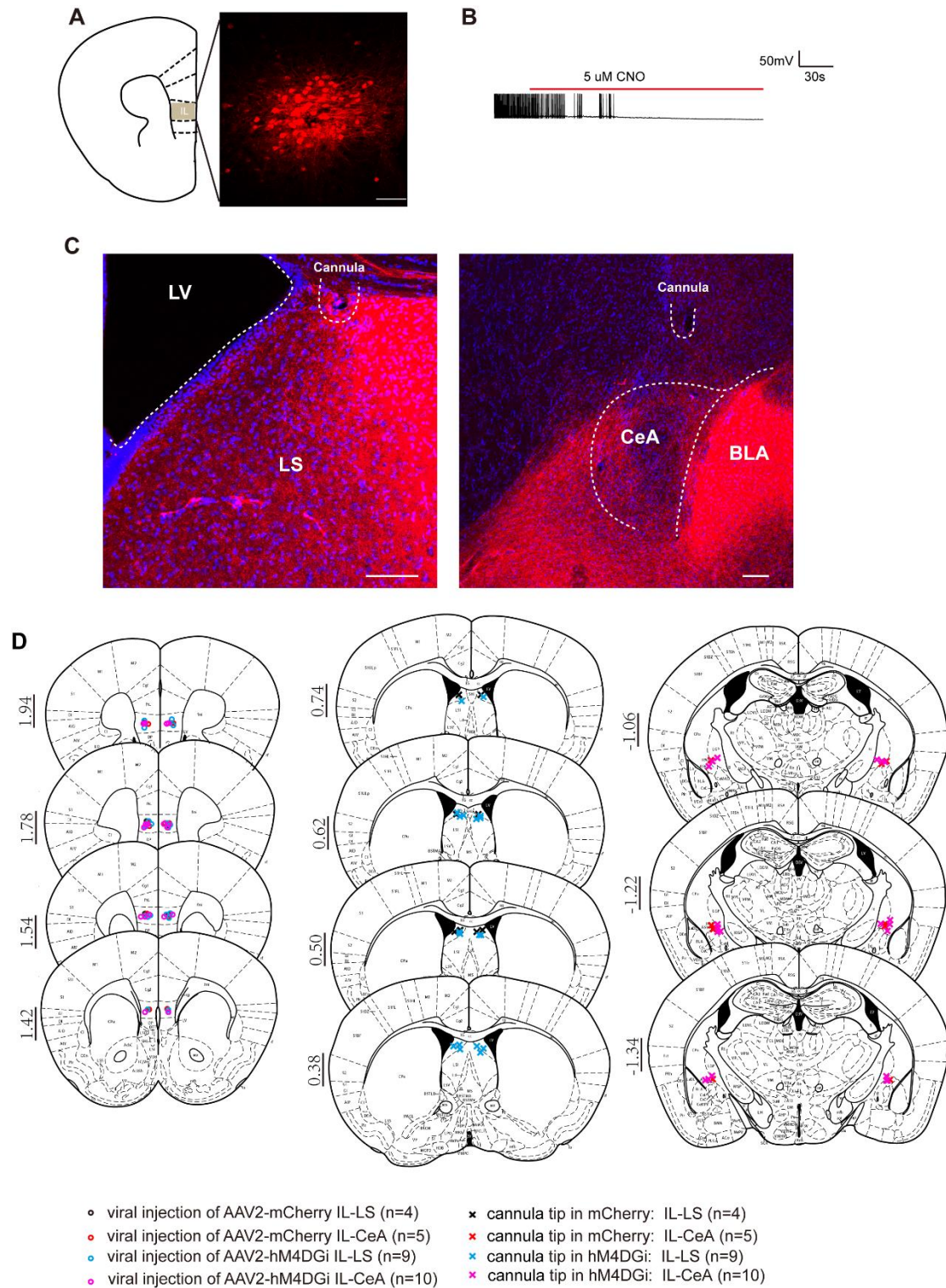
BLA. **C-F**, Activation of BLA terminals had no effects in the EPM ($n = 8,9$ mice for eYFP and Chr2; **C**, $F_{\text{interaction}}(2,30) = 1.205$, $p = 0.3138$; **D**, $F_{\text{interaction}}(2,30) = 0.4929$, $p = 0.6157$) or OFT (**E**, $F_{\text{interaction}}(2,30) = 0.7819$, $p = 0.4666$; **F**, $F_{\text{interaction}}(2,30) = 0.0523$, $p = 0.6938$). **G**, Histologically verified placement of viral injections and optic fibres in the Chr2 and eYFP groups for IL–BLA projections. **H**, eYFP and Chr2 mice expressing eYFP or Chr2-eYFP, respectively, in the IL with optic fibres above the BNST. **I-L**, activation of BNST terminals had no effects in the EPM ($n = 12$ and 12 mice for eYFP and Chr2, **I**, $F_{\text{interaction}}(2,44) = 0.0523$, $p = 0.9490$; **J**, $F_{\text{interaction}}(2,44) = 0.4984$, $p = 0.6109$) and OFT (**K**, $F_{\text{interaction}}(2,44) = 0.1886$, $p = 0.8287$; **L**, $F_{\text{interaction}}(2,44) = 0.3683$, $p = 0.6940$). **M**, Histologically verified placement of viral injections and optic fibres in the Chr2 and eYFP groups for the IL–BNST projections. Scale bar represents $100\ \mu\text{m}$. Statistics in **C-F** and **I-L** reflect two-way repeated-measures ANOVA with Bonferroni post hoc analysis. Data show the mean \pm S.E.M. See Supplemental Table 1 for statistical details.



Supplementary Figure 6 Histologically verified placement of viral injections and cannula in the saline and AP5+CNQX groups. Related to Figure 3. **A**, Left, centre of the viral injection in the IL for all of the animals analysed in Figure 3C-F; right, location of the cannula above the LS for all of the animals analysed in Figure 4C-F. **B**, Left, centre of the viral injection in the IL for all of the animals analysed in Figure 4H-K; right, location of the cannula above the CeA for all of the animals analysed in Figure 4H-K. Scale bar represents 100 μ m.

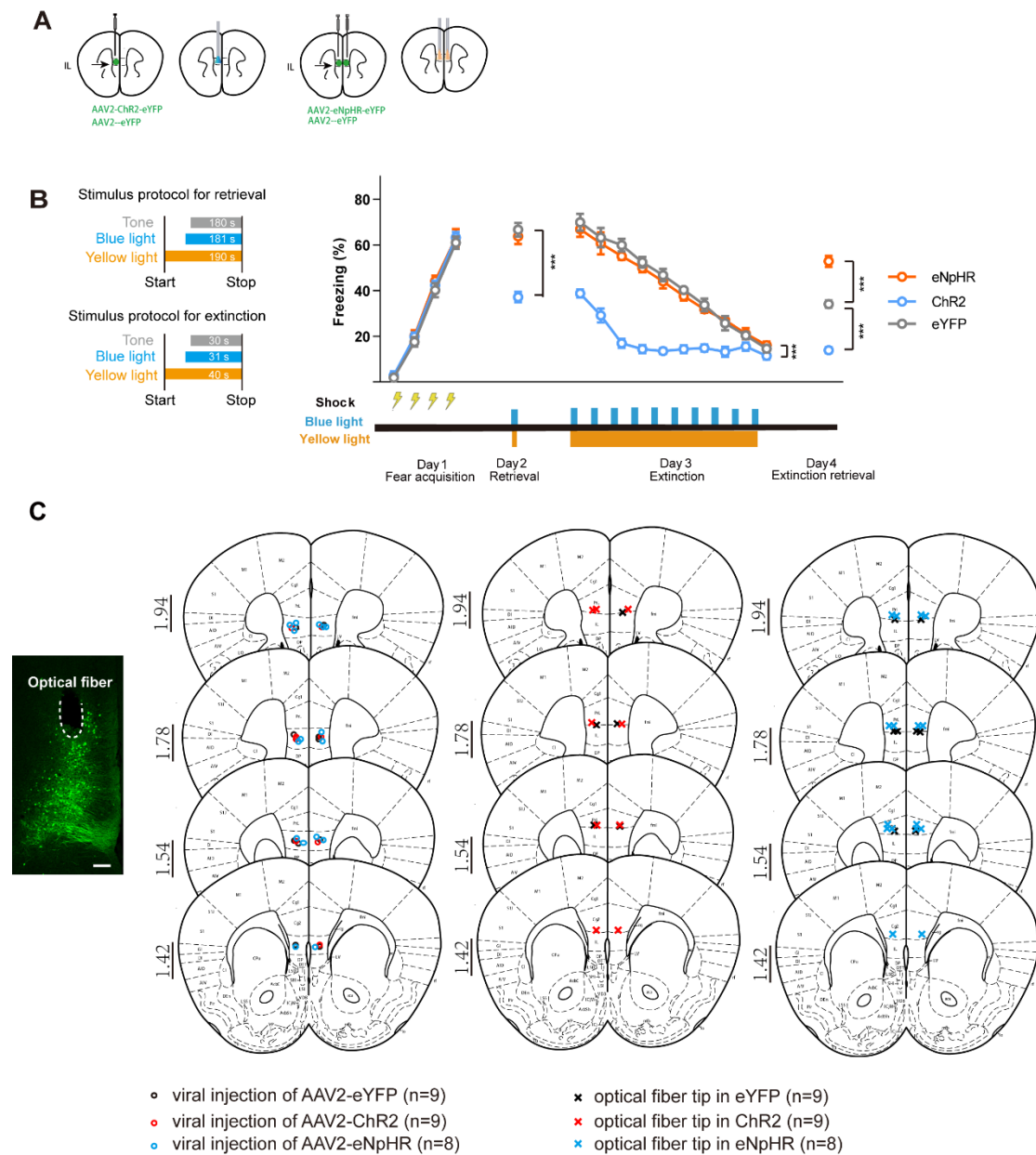


Supplementary Figure 7 Histologically verified placement of viral injections and optic fibres in the eNpHR and eYFP groups. Related to Figure 5. Left, centre of the viral injection in the IL for all of the animals analysed in Figure 5B-E; middle, location of the optic fibre above the LS for all of the animals analysed in Figure 5B-E; right, location of the optic fibre tip above the CeA for all of the animals analysed in Figure 5B-E. Scale bar represents 100 μ m.



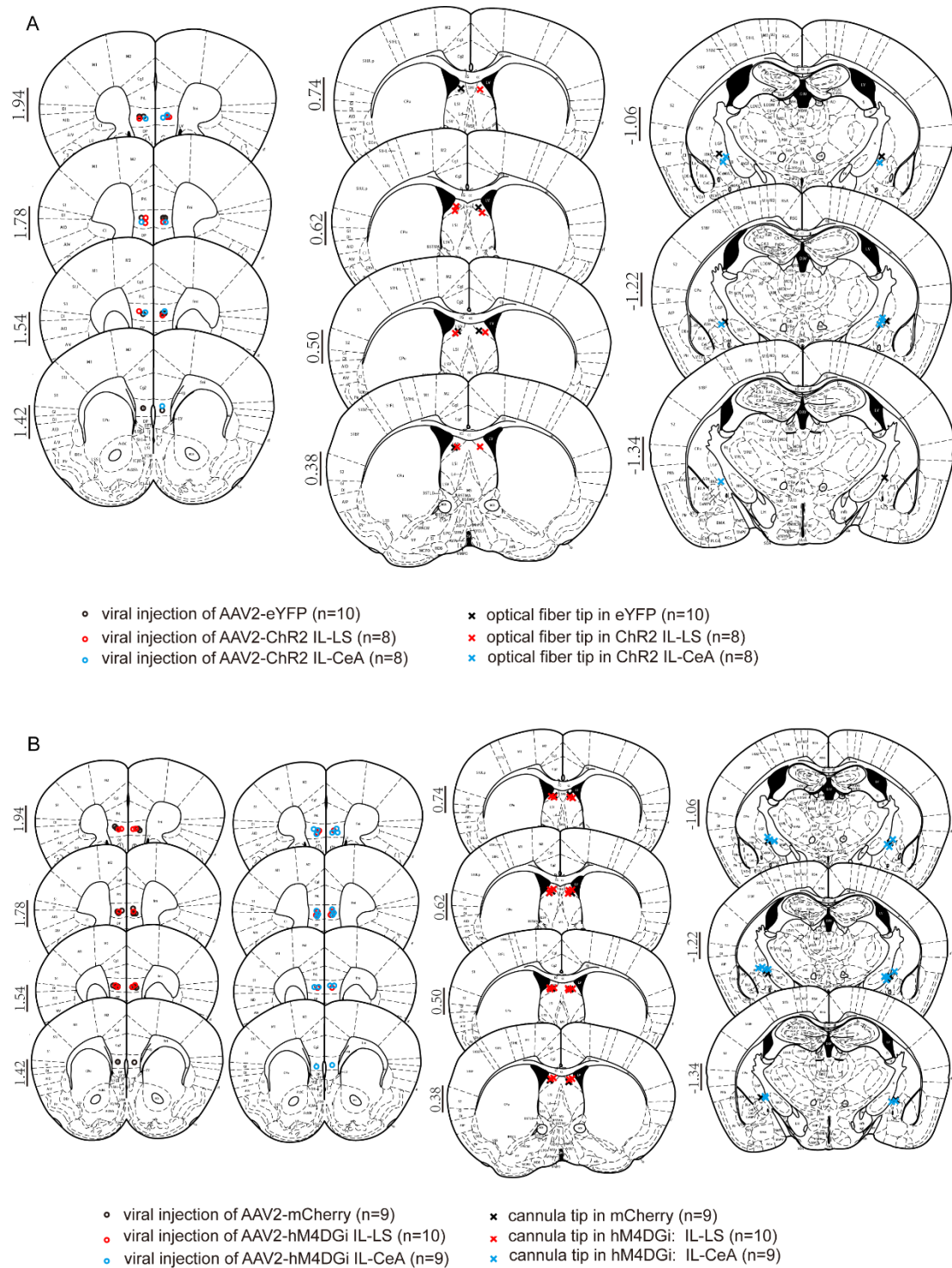
Supplementary Figure 8 Validation of hM4DGi and histologically verified placement of viral injections and optic fibres in the hM4DGi and mCherry groups. Related to Figure 5. **A**, Expression of hM4DGi-mCherry in the IL; scale bar: 100 μ m. **B**, CNO treatment blocked evoked spiking of hM4DGi cells in the IL. **C**, Representative images for optical fibre implantation and mCherry expression in the LS (left) and CeA (right).

D, Left, centre of the viral injection in the IL for all of the animals analysed in Figure 5G-J; middle, location of the optic fibre above the LS for all of the animals analysed in Figure 5G-J; left, location of the optic fibre tip above the CeA for all of the animals analysed in Figure 5G-J. Scale bar represents 100 μm .



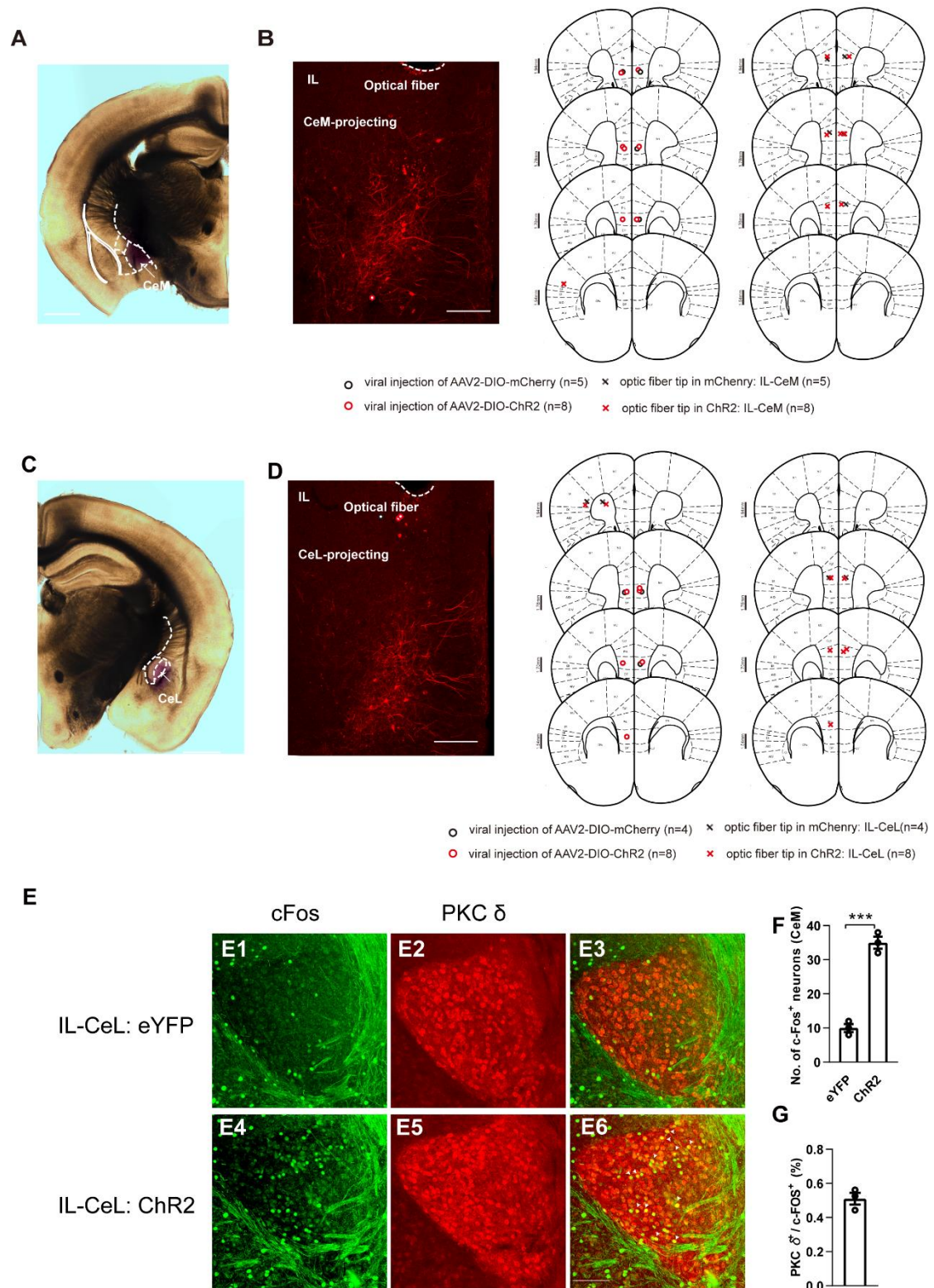
Supplementary Figure 9 IL regulates fear extinction. **A**, Mice expressing opsin or eYFP in the IL with optic fibres above the IL. **B**, Effects of optogenetic manipulation of the IL on fear retrieval and fear extinction. Optogenetic activation of IL neurons reduced fear retrieval ($F(2,21) = 32.07, p < 0.0001$), reduced extinction ($F_{\text{Interaction}}(18,189) = 9.718, p < 0.0001$) and facilitated extinction retrieval ($F(2,21) = 112.4, p < 0.0001$). Optogenetic silencing of IL during extinction tones did not affect fear expression but impaired retrieval of extinction the following day. **C**, Centre of the viral injection and location of the optic fibre. Scale bar represents 100 μm . $n = 8, 8$, and 8 mice for eYFP, ChR2 and eNpHR. One-way ANOVA with Dunnett's multiple comparisons test for fear retrieval and extinction retrieval and two-way repeated-measures ANOVA with Dunnett's

multiple comparisons test for fear extinction. Data show the mean \pm S.E.M. See Supplemental Table 1 for statistical details.



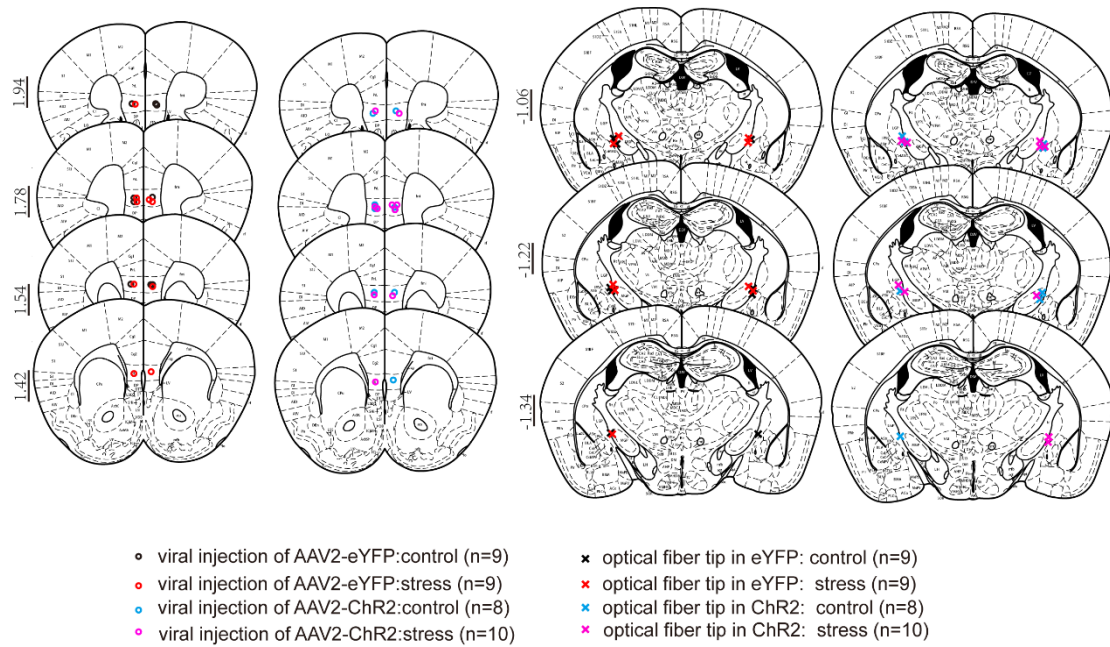
Supplementary Figure 10 Histologically verified placement of viral injections and optic fibres. Related to Figure 6. **A**, Left, centre of the viral injection in the IL for all of the animals analysed in Figure 7B; middle, location of the optic fibre above the LS for all of the animals analysed in Figure 7B; right, location of the optic fibre tip above the CeA for all of the animals analysed in Figure 7B. **B**, Left, centre of the viral injection in the IL for all of the animals analysed in Figure 7D; middle, location of the optic fibre

above the LS for all of the animals analysed in Figure 7D; right, location of the optic fibre tip above the CeA for all of the animals analysed in Figure 7D.



Supplementary Figure 11 Light stimulation-induced c-Fos expression in both PKC- δ^+ and PKC- δ^- neurons and histologically verified placement of viral injections and optic fibres. Related to Figure 7. **A**, Representative image showing the spread of trypan blue in the CeM (as indicated by the arrow). **B**, Centre of the viral injection and location of

the optic fibre tip for stimulating CeM-projecting IL neurons. **C**, Representative image showing the spread of trypan blue in the CeL (as indicated by the arrow). **D**, Centre of the viral injection and location of the optic fibre tip for stimulating CeM-projecting IL neurons. **E**, Representative images showing light stimulation-induced c-Fos expression in both PKC- δ^+ and PKC- δ^- neurons. **F**, Increased c-Fos expression in the CeL of IL-CeL:Chr2 mice following activation of CeL-projecting IL neurons. **G**, c-Fos expressed in both PKC- δ^+ and PKC- δ^- neurons. Three mice per group, 4 slices for each mouse. **A,C**, Scale bar represents 1000 μm . **E**, Scale bar represents 200 μm .



Supplementary Figure 12 Histologically verified placement of viral injections and optic fibres. Related to Figure 8. Left two columns, centre of the viral injection in the IL for all of the animals analysed in Figure 8; right two columns, location of the optic fiber tip above the CeA for all of the animals analysed in Figure 8.

Supplemental Table 1

Figure 1		sample size (fugire order)		Treatment effect		significance
E	eYFP vs Chr2	mice = 10,8	two-way repeated measures ANOVA	group×epoch interaction F (2, 32) = 3.959	$P = 0.0291$	$p < 0.05$
	OFF		Bonferroni's multiple comparisons test	t = 0.74, df = 13.01	$p > 0.9999$	<i>n.s.</i>
	ON		Bonferroni's multiple comparisons test	t = 5.29, df = 13.48	$p = 0.0004$	$p < 0.001$
	OFF		Bonferroni's multiple comparisons test	t = 6.52, df = 15.97	$p < 0.0001$	$p < 0.001$
F	eYFP vs Chr2	mice = 10,8	two-way repeated measures ANOVA	group×epoch interaction F (2, 32) = 10.88	$P = 0.0002$	$p < 0.001$
	OFF		Bonferroni's multiple comparisons test	t = 0.86, df = 11.82	$p > 0.9999$	<i>n.s.</i>
	ON		Bonferroni's multiple comparisons test	t = 5.88, df = 12.96	$p = 0.0002$	$p < 0.001$
	OFF		Bonferroni's multiple comparisons test	t = 8.20, df = 14.91	$p < 0.0001$	$p < 0.001$
H	eYFP vs Chr2	mice = 10,8	two-way repeated measures ANOVA	group×epoch interaction F (2, 32) = 21.12	$p < 0.0001$	$p < 0.001$
	OFF		Bonferroni's multiple comparisons test	t = 1.01, df = 15.86	$p = 0.9785$	<i>n.s.</i>
	ON		Bonferroni's multiple comparisons test	t = 7.84, df = 14.11	$p < 0.0001$	$p < 0.001$
	OFF		Bonferroni's multiple comparisons test	t = 6.97, df = 15.09	$p < 0.0001$	$p < 0.001$
I	eYFP vs Chr2	mice = 10,8	two-way repeated measures ANOVA	group×epoch interaction F (2, 32) = 0.6094	$P = 0.5499$	<i>n.s.</i>
M	eYFP vs eNpHR	mice = 7,7	two-way repeated measures ANOVA	group×epoch interaction F (2, 24) = 4.452	$P = 0.0227$	$p < 0.05$
	OFF		Bonferroni's multiple comparisons test	t = 0.20, df = 11.91	$p > 0.9999$	<i>n.s.</i>
	ON		Bonferroni's multiple comparisons test	t = 4.29, df = 11.98	$p = 0.0032$	$p < 0.01$
	OFF		Bonferroni's multiple comparisons test	t = 0.39, df = 11.97	$p > 0.9999$	<i>n.s.</i>
N	eYFP vs eNpHR	mice = 7,7	two-way repeated measures ANOVA	group×epoch interaction F (2, 24) = 7.726	$P = 0.0026$	$p < 0.01$
	OFF		Bonferroni's multiple comparisons test	t = 0.52, df = 11.02	$p > 0.9999$	<i>n.s.</i>
	ON		Bonferroni's multiple comparisons test	t = 3.61, df = 8.66	$p = 0.0181$	$p < 0.05$
	OFF		Bonferroni's multiple comparisons test	t = 1.08, df = 11.34	$p = 0.9098$	<i>n.s.</i>
O	eYFP vs eNpHR	mice = 7,7	two-way repeated measures ANOVA	group×epoch interaction F (2, 24) = 11.76	$p < 0.0003$	$p < 0.001$
	OFF		Bonferroni's multiple comparisons test	t = 1.06, df = 9.63	$p = 0.9432$	<i>n.s.</i>
	ON		Bonferroni's multiple comparisons test	t = 5.94, df = 11.49	$p < 0.0002$	$p < 0.001$
	OFF		Bonferroni's multiple comparisons test	t = 3.27, df = 10.15	$p = 0.0248$	$p < 0.05$
P	eYFP vs eNpHR	mice = 7,7	two-way repeated measures ANOVA	group×epoch interaction F (2, 24) = 0.05753	$P = 0.9442$	<i>n.s.</i>
Figure 2						
E	eYFP vs Chr2	mice = 15,13	two-way repeated measures ANOVA	group×epoch interaction F (2, 52) = 8.447	$P = 0.0007$	$p < 0.001$
	OFF		Bonferroni's multiple comparisons test	t = 0.08, df = 23.19	$p > 0.9999$	<i>n.s.</i>
	ON		Bonferroni's multiple comparisons test	t = 6.65, df = 20.64	$p < 0.0001$	$p < 0.001$
	OFF		Bonferroni's multiple comparisons test	t = 3.07, df = 25.34	$p = 0.0152$	$p < 0.05$
F	eYFP vs Chr2	mice = 15,13	two-way repeated measures ANOVA	group×epoch interaction F (2, 52) = 11.35	$P = 0.0002$	$p < 0.001$
	OFF		Bonferroni's multiple comparisons test	t = 0.59, df = 24.18	$p > 0.9999$	<i>n.s.</i>
	ON		Bonferroni's multiple comparisons test	t = 5.21, df = 25.99	$p < 0.0001$	$p < 0.001$
	OFF		Bonferroni's multiple comparisons test	t = 4.78, df = 25.41	$p = 0.0002$	$p < 0.001$
G	eYFP vs Chr2	mice = 15,13	two-way repeated measures ANOVA	group×epoch interaction F (2, 52) = 11.90	$p < 0.0001$	$p < 0.001$
	OFF		Bonferroni's multiple comparisons test	t = 0.01, df = 25.22	$p > 0.9999$	<i>n.s.</i>
	ON		Bonferroni's multiple comparisons test	t = 6.09, df = 26.00	$p < 0.0001$	$p < 0.001$
	OFF		Bonferroni's multiple comparisons test	t = 0.45, df = 25.26	$p > 0.9999$	<i>n.s.</i>
H	eYFP vs Chr2	mice = 15,13	two-way repeated measures ANOVA	group×epoch interaction F (2, 52) = 0.1149	$P = 0.8917$	<i>n.s.</i>
J	eYFP vs Chr2	mice = 8,8	two-way repeated measures ANOVA	group×epoch interaction F (2, 28) = 7.200	$P = 0.0030$	$p < 0.01$
	OFF		Bonferroni's multiple comparisons test	t = 0.58, df = 11.75	$p > 0.9999$	<i>n.s.</i>
	ON		Bonferroni's multiple comparisons test	t = 4.02, df = 12.62	$p = 0.0046$	$p < 0.01$
	OFF		Bonferroni's multiple comparisons test	t = 0.37, df = 13.27	$p > 0.9999$	<i>n.s.</i>
K	eYFP vs Chr2	mice = 8,8	two-way repeated measures ANOVA	group×epoch interaction F (2, 28) = 7.264	$P = 0.0029$	$p < 0.01$
	OFF		Bonferroni's multiple comparisons test	t = 0.72, df = 13.47	$p > 0.9999$	<i>n.s.</i>
	ON		Bonferroni's multiple comparisons test	t = 4.16, df = 13.61	$P = 0.0030$	$p < 0.01$
	OFF		Bonferroni's multiple comparisons test	t = 0.42, df = 13.83	$p > 0.9999$	<i>n.s.</i>
L	eYFP vs Chr2	mice = 8,8	two-way repeated measures ANOVA	group×epoch interaction F (2, 28) = 12.18	$P = 0.0002$	$p < 0.001$
	OFF		Bonferroni's multiple comparisons test	t = 0.46, df = 13.65	$p > 0.9999$	<i>n.s.</i>
	ON		Bonferroni's multiple comparisons test	t = 6.12, df = 11.61	$P = 0.0002$	$p < 0.001$
	OFF		Bonferroni's multiple comparisons test	t = 0.24, df = 13.65	$p > 0.9999$	<i>n.s.</i>
M	eYFP vs Chr2	mice = 8,8	two-way repeated measures ANOVA	group×epoch interaction F (2, 28) = 0.3525	$P = 0.7060$	<i>n.s.</i>
Figure 3						
C	Saline vs AP5+NB	mice = 13,11	two-way repeated measures ANOVA	group×epoch interaction F (2, 44) = 12.57	$p < 0.0001$	$p < 0.001$
	OFF		Bonferroni's multiple comparisons test	t = 0.73, df = 21.85	$p > 0.9999$	<i>n.s.</i>
	ON		Bonferroni's multiple comparisons test	t = 6.39, df = 16.53	$p < 0.0001$	$p < 0.001$
	OFF		Bonferroni's multiple comparisons test	t = 0.39, df = 17.07	$p > 0.9999$	<i>n.s.</i>
D	Saline vs AP5+NB	mice = 13,11	two-way repeated measures ANOVA	group×epoch interaction F (2, 44) = 17.71	$p < 0.0001$	$p < 0.001$
	OFF		Bonferroni's multiple comparisons test	t = 0.51, df = 21.98	$p > 0.9999$	<i>n.s.</i>
	ON		Bonferroni's multiple comparisons test	t = 7.02, df = 14.77	$p < 0.0001$	$p < 0.001$
	OFF		Bonferroni's multiple comparisons test	t = 0.79, df = 21.99	$p > 0.9999$	<i>n.s.</i>
E	Saline vs AP5+NB	mice = 9,8	two-way repeated measures ANOVA	group×epoch interaction F (2, 30) = 3.392	$P = 0.0470$	$p < 0.05$
	OFF		Bonferroni's multiple comparisons test	t = 1.05, df = 14.61	$P = 0.9297$	<i>n.s.</i>
	ON		Bonferroni's multiple comparisons test	t = 5.15, df = 12.34	$P = 0.0007$	$p < 0.001$
	OFF		Bonferroni's multiple comparisons test	t = 0.89, df = 14.71	$p > 0.9999$	<i>n.s.</i>
F	Saline vs AP5+NB	mice = 9,8	two-way repeated measures ANOVA	group×epoch interaction F (2, 30) = 0.2107	$P = 0.8112$	<i>n.s.</i>

H	Saline vs AP5+NB	mice = 11,10	two-way repeated measures ANOVA	group×epoch interaction F (2, 38) = 3.100	$P = 0.0566$	<i>n.s.</i>
	OFF		Bonferroni's multiple comparisons test	$t = 0.13$, $df = 18.96$	$p > 0.9999$	<i>n.s.</i>
	ON		Bonferroni's multiple comparisons test	$t = 2.79$, $df = 18.80$	$p < 0.0356$	$p < 0.05$
	OFF		Bonferroni's multiple comparisons test	$t = 0.01$, $df = 18.89$	$p > 0.9999$	<i>n.s.</i>
I	Saline vs AP5+NB	mice = 11,10	two-way repeated measures ANOVA	group×epoch interaction F (2, 38) = 13.84	$p < 0.0001$	$p < 0.001$
	OFF		Bonferroni's multiple comparisons test	$t = 0.50$, $df = 19.00$	$p > 0.9999$	<i>n.s.</i>
	ON		Bonferroni's multiple comparisons test	$t = 5.73$, $df = 15.99$	$p < 0.0001$	$p < 0.001$
	OFF		Bonferroni's multiple comparisons test	$t = 0.58$, $df = 18.95$	$p > 0.9999$	<i>n.s.</i>
J	Saline vs AP5+NB	mice = 10,9	two-way repeated measures ANOVA	group×epoch interaction F (2, 34) = 7.009	$P = 0.0028$	$p < 0.01$
	OFF		Bonferroni's multiple comparisons test	$t = 0.28$, $df = 12.51$	$p > 0.9999$	<i>n.s.</i>
	ON		Bonferroni's multiple comparisons test	$t = 2.80$, $df = 14.06$	$P = 0.0424$	$p < 0.05$
	OFF		Bonferroni's multiple comparisons test	$t = 2.04$, $df = 16.73$	$P = 0.1712$	<i>n.s.</i>
K	Saline vs AP5+NB	mice = 10,9	two-way repeated measures ANOVA	group×epoch interaction F (2, 34) = 0.08985	$P = 0.7863$	<i>n.s.</i>
Figure 4						
I		$n = 7$ neurons from 2 mice	one-way ANOVA	F (3, 24) = 27.01	$P < 0.0001$	$p < 0.001$
	ACSF vs TTX		Tukey's multiple comparisons test	$q = 10.39$, $df = 24$	$P < 0.0001$	$p < 0.001$
	ACSF vs TTX+4AP		Tukey's multiple comparisons test	$q = 3.64$, $df = 24$	$P = 0.0740$	<i>n.s.</i>
	TTX vs TTX+4AP		Tukey's multiple comparisons test	$q = 6.76$, $df = 24$	$P = 0.0004$	$p < 0.001$
	TTX+4AP vs TTX+4AP+CNQX		Tukey's multiple comparisons test	$q = 6.86$, $df = 24$	$P = 0.0003$	$p < 0.001$
M		$n = 5$ neurons from 2 mice	one-way ANOVA	F (3, 16) = 26.54	$P < 0.0001$	$p < 0.001$
	ACSF vs TTX		Tukey's multiple comparisons test	$q = 10.39$, $df = 24$	$P < 0.0001$	$p < 0.001$
	ACSF vs TTX+4AP		Tukey's multiple comparisons test	$q = 3.64$, $df = 24$	$P = 0.1212$	<i>n.s.</i>
	TTX vs TTX+4AP		Tukey's multiple comparisons test	$q = 6.76$, $df = 24$	$P = 0.0008$	$p < 0.001$
	TTX+4AP vs TTX+4AP+CNQX		Tukey's multiple comparisons test	$q = 6.86$, $df = 24$	$P = 0.0009$	$p < 0.001$
Figure 5						
B	eYFP_eNpHR-LS_e	mice = 8,7,7	two-way repeated measures ANOVA	group×epoch interaction F (4, 38) = 15.69	$p < 0.0001$	$p < 0.001$
	OFF		Dunnett's multiple comparisons test			
	eYFP vs. eNpHR-LS			$q = 0.55$, $df = 10.93$	$P = 0.8098$	<i>n.s.</i>
	eYFP vs. eNpHR-CeA			$q = 0.40$, $df = 10.96$	$P = 0.9988$	<i>n.s.</i>
	ON		Dunnett's multiple comparisons test			
	eYFP vs. eNpHR-LS			$q = 6.65$, $df = 12.93$	$p < 0.0001$	$p < 0.001$
	eYFP vs. eNpHR-CeA			$q = 3.54$, $df = 10.72$	$P = 0.0090$	$p < 0.01$
	OFF		Dunnett's multiple comparisons test			
	eYFP vs. eNpHR-LS			$q = 0.42$, $df = 13.00$	$P = 0.8840$	<i>n.s.</i>
	eYFP vs. eNpHR-CeA			$q = 0.15$, $df = 12.48$	$P = 0.9833$	<i>n.s.</i>
C	eYFP_eNpHR-LS_e	mice = 8,7,7	two-way repeated measures ANOVA	group×epoch interaction F (4, 38) = 17.89	$p < 0.0001$	$p < 0.001$
	OFF		Dunnett's multiple comparisons test			
	eYFP vs. eNpHR-LS			$q = 0.13$, $df = 12.93$	$P = 0.9883$	<i>n.s.</i>
	eYFP vs. eNpHR-CeA			$q = 0.91$, $df = 12.96$	$P = 0.5795$	<i>n.s.</i>
	ON		Dunnett's multiple comparisons test			
	eYFP vs. eNpHR-LS			$q = 2.82$, $df = 7.84$	$P = 0.0413$	$p < 0.05$
	eYFP vs. eNpHR-CeA			$q = 6.91$, $df = 12.20$	$p < 0.0001$	$p < 0.001$
	OFF		Dunnett's multiple comparisons test			
	eYFP vs. eNpHR-LS			$q = 0.09$, $df = 12.57$	$P = 0.9939$	<i>n.s.</i>
	eYFP vs. eNpHR-CeA			$q = 0.33$, $df = 12.74$	$P = 0.9244$	<i>n.s.</i>
D	eYFP_eNpHR-LS_e	mice = 8,7,7	two-way repeated measures ANOVA	group×epoch interaction F (4, 38) = 18.38	$p < 0.0001$	$p < 0.001$
	OFF		Dunnett's multiple comparisons test			
	eYFP vs. eNpHR-LS			$q = 0.70$, $df = 12.62$	$P = 0.7171$	<i>n.s.</i>
	eYFP vs. eNpHR-CeA			$q = 0.27$, $df = 13.00$	$P = 0.9482$	<i>n.s.</i>
	ON		Dunnett's multiple comparisons test			
	eYFP vs. eNpHR-LS			$q = 6.24$, $df = 10.48$	$P = 0.0002$	$p < 0.001$
	eYFP vs. eNpHR-CeA			$q = 5.04$, $df = 12.08$	$P = 0.0002$	$p < 0.001$
	OFF		Dunnett's multiple comparisons test			
	eYFP vs. eNpHR-LS			$q = 1.04$, $df = 12.41$	$P = 0.4980$	<i>n.s.</i>
	eYFP vs. eNpHR-CeA			$q = 0.37$, $df = 12.37$	$P = 0.9086$	<i>n.s.</i>
E	eYFP_eNpHR-LS_e	mice = 8,7,7	two-way repeated measures ANOVA	group×epoch interaction F (4, 38) = 0.1215	$P = 0.9740$	<i>n.s.</i>
G	mCherry_Gi-LS_G	mice = 9,10,9	one-way ANOVA	F (2, 25) = 32.10	$P < 0.0001$	$P < 0.001$
	mCherry vs. Gi-LS		Dunnett's multiple comparisons test	$q = 4.29$, $df = 25$		$p < 0.001$
	mCherry vs. Gi-CeA		Dunnett's multiple comparisons test	$q = 3.61$, $df = 25$		$p < 0.01$
H	mCherry_Gi-LS_G	mice = 9,10,9	one-way ANOVA	F (2, 25) = 36.92	$P < 0.0001$	$P < 0.001$
	mCherry vs. Gi-LS		Dunnett's multiple comparisons test	$q = 4.45$, $df = 25$	$P = 0.0003$	$p < 0.001$
	mCherry vs. Gi-CeA		Dunnett's multiple comparisons test	$q = 4.02$, $df = 25$	$P = 0.0009$	$p < 0.001$
I	mCherry_Gi-LS_G	mice = 9,10,9	one-way ANOVA	F (2, 25) = 80.83	$P < 0.0001$	$P < 0.001$
	mCherry vs. Gi-LS		Dunnett's multiple comparisons test	$q = 7.81$, $df = 25$		$p < 0.001$
	mCherry vs. Gi-CeA		Dunnett's multiple comparisons test	$q = 4.61$, $df = 25$		$p < 0.001$
J	mCherry_Gi-LS_G	mice = 9,10,9	one-way ANOVA	F (2, 25) = 0.8084	$P = 0.4569$	<i>n.s.</i>
Figure 6						
B	eYFP_Chr2-LS_C	mice = 10,8,8	one-way ANOVA	F (2, 23) = 0.04646	$P = 0.9547$	<i>n.s.</i>
	retrival					
	fear extinction		two-way repeated measures ANOVA	F (18, 207) = 3.540	$P < 0.0001$	$P < 0.001$
	eYFP vs Chr2-LS		Dunnett's multiple comparisons test	$q = 3.49$, $df = 188.0$	$P = 0.0012$	$p < 0.01$
	eYFP vs Chr2-CeA		Dunnett's multiple comparisons test	$q = 5.06$, $df = 166.4$	$P < 0.0001$	$p < 0.001$
	extinction retrival		one-way ANOVA	F (2, 23) = 17.23	$P < 0.0001$	$P < 0.001$
	eYFP vs Chr2-LS		Dunnett's multiple comparisons test	$q = 2.69$, $df = 23$	$P = 0.0249$	$p < 0.05$
	eYFP vs Chr2-CeA		Dunnett's multiple comparisons test	$q = 3.48$, $df = 23$	$P = 0.0039$	$p < 0.01$
D	mCherry_Gi-LS_G	mice = 9,10,9	one-way ANOVA	F (2, 25) = 0.4312	$P = 0.6545$	<i>n.s.</i>
	retrival		one-way ANOVA	F (2, 25) = 0.4312	$P = 0.6545$	<i>n.s.</i>
	fear extinction		two-way repeated measures ANOVA	F (18, 230) = 3.336	$P < 0.0001$	$P < 0.001$
	mCherry vs Gi-LS		Dunnett's multiple comparisons test	$q = 9.03$, $df = 230$	$P < 0.0001$	$p < 0.01$
	mCherry vs Gi-CeA		Dunnett's multiple comparisons test	$q = 5.80$, $df = 230$	$P < 0.0001$	$p < 0.001$
	extinction retrival		one-way ANOVA	F (2, 25) = 25.88	$P < 0.0001$	$P < 0.001$
	mCherry vs Gi-LS		Dunnett's multiple comparisons test	$q = 3.96$, $df = 25$	$P = 0.0011$	$p < 0.01$
	mCherry vs Gi-CeA		Dunnett's multiple comparisons test	$q = 3.13$, $df = 25$	$P = 0.0084$	$p < 0.01$
Figure 7						
F	mCherry_Chr2-Ce	mice = 9,8,8	two-way repeated measures ANOVA	group×epoch interaction F (4, 38) = 15.69	$p < 0.0001$	$p < 0.001$
	OFF		Dunnett's multiple comparisons test			
	mCherry vs Chr2-CeL			$q = 0.55$, $df = 10.93$	$P = 0.8098$	<i>n.s.</i>
	mCherry vs Chr2-CeM			$q = 0.40$, $df = 10.96$	$P = 0.9988$	<i>n.s.</i>
	ON		Dunnett's multiple comparisons test			
	mCherry vs Chr2-CeL			$q = 6.65$, $df = 12.93$	$p < 0.0001$	$p < 0.001$
	mCherry vs Chr2-CeM			$q = 3.54$, $df = 10.72$	$P = 0.0090$	$p < 0.01$
	OFF		Dunnett's multiple comparisons test			

	mCherry vs ChR2-CeL		q = 0.42, df = 13.00	P = 0.8840	n.s.
	mCherry vs ChR2-CeM		q = 0.15, df = 12.48	P = 0.9833	n.s.
G	mCherry,ChR2-Ce mice = 9,8,8	two-way repeated measures ANOVA	group×epoch interaction F (4, 38) = 17.89	p < 0.0001	p < 0.001
	OFF	Dunnett's multiple comparisons test			
	mCherry vs ChR2-CeL		q = 0.13, df = 12.93	P = 0.9883	n.s.
	mCherry vs ChR2-CeM		q = 0.91, df = 12.96	P = 0.5795	n.s.
	ON	Dunnett's multiple comparisons test			
	mCherry vs ChR2-CeL		q = 2.82, df = 7.84	P = 0.0413	p < 0.05
	mCherry vs ChR2-CeM		q = 6.91, df = 12.20	p < 0.0001	p < 0.001
	OFF	Dunnett's multiple comparisons test			
	mCherry vs ChR2-CeL		q = 0.09, df = 12.57	P = 0.9939	n.s.
	mCherry vs ChR2-CeM		q = 0.33, df = 12.74	P = 0.9244	n.s.
H	mCherry,ChR2-Ce mice = 9,8,8	two-way repeated measures ANOVA	group×epoch interaction F (4, 38) = 18.38	p < 0.0001	p < 0.001
	OFF	Dunnett's multiple comparisons test			
	mCherry vs ChR2-CeL		q = 0.70, df = 12.62	P = 0.7171	n.s.
	mCherry vs ChR2-CeM		q = 0.27, df = 13.00	P = 0.9482	n.s.
	ON	Dunnett's multiple comparisons test			
	mCherry vs ChR2-CeL		q = 6.24, df = 10.48	P = 0.0002	p < 0.001
	mCherry vs ChR2-CeM		q = 5.04, df = 12.08	P = 0.0002	p < 0.001
	OFF	Dunnett's multiple comparisons test			
	mCherry vs ChR2-CeL		q = 1.04, df = 12.41	P = 0.4980	n.s.
	mCherry vs ChR2-CeM		q = 0.37, df = 12.37	P = 0.9086	n.s.
I	mCherry,ChR2-Ce mice = 9,8,8	two-way repeated measures ANOVA	group×epoch interaction F (4, 38) = 0.1215	P = 0.9740	n.s.

J	mCherry ChR2-Ce mice = 9,8,8				
	retrial	one-way ANOVA	F (2, 22) = 0.1155	P = 0.8914	n.s.
	fear extinction	two-way repeated measures ANOVA	group F (2,20) = 13.51	P = 0.0002	P < 0.001
	mCherry vs ChR2-CeL	Dunnett's multiple comparisons test	q = 0.4726, df = 155.9	P = 0.8523	n.s.
	mCherry vs ChR2-CeM	Dunnett's multiple comparisons test	q = 2.892, df = 143.1	P = 0.0086	p < 0.01
	extinction retrieval	one-way ANOVA	F (2, 22) = 45.12	P < 0.0001	P < 0.001
	mCherry vs ChR2-CeL	Dunnett's multiple comparisons test	q = 1.302, df = 22	P = 0.3430	n.s.
	mCherry vs ChR2-CeM	Dunnett's multiple comparisons test	q = 7.69, df = 22	P < 0.0001	P < 0.001

Figure 8					
B	Con-eYFP, Stress: mice = 9,9,9,8	two-way repeated measures ANOVA	group×epoch interaction F (6, 63) = 8.890	p < 0.0001	p < 0.001
	OFF	Tukey's multiple comparisons test			
	Con-eYFP vs. Stress-eYFP		q = 6.28, df = 15.99	P = 0.0021	p < 0.01
	Con-eYFP vs. Con-ChR2		q = 0.63, df = 14.97	P = 0.9688	n.s.
	Stress-eYFP vs. Stress-ChR2		q = 0.16, df = 16.61	P = 0.9994	n.s.
	Con-ChR2 vs. Stress-ChR2		q = 6.48, df = 15.91	P < 0.0016	p < 0.01
	ON	Tukey's multiple comparisons test			
	Con-eYFP vs. Stress-eYFP		q = 6.27, df = 15.43	P = 0.0023	p < 0.01
	Con-eYFP vs. Con-ChR2		q = 6.78, df = 13.77	P = 0.0015	p < 0.01
	Stress-eYFP vs. Stress-ChR2		q = 9.38, df = 16.17	P < 0.0001	p < 0.001
	Con-ChR2 vs. Stress-ChR2		q = 3.60, df = 14.40	P = 0.0940	n.s.
	OFF	Tukey's multiple comparisons test			

	Con-eYFP vs. Stress-eYFP		q = 8.32, df = 16.00	P = 0.0001	p < 0.001
	Con-eYFP vs. Con-ChR2		q = 0.19, df = 14.83	P = 0.9992	n.s.
	Stress-eYFP vs. Stress-ChR2		q = 1.38, df = 12.98	P = 0.7637	n.s.
	Con-ChR2 vs. Stress-ChR2		q = 4.44, df = 13.15	P = 0.0345	p < 0.05
C	Con-eYFP, Stress: mice = 9,9,9,8	two-way repeated measures ANOVA	group×epoch interaction F (6, 64) = 11.40	p < 0.0001	p < 0.001
	OFF	Tukey's multiple comparisons test			
	Con-eYFP vs. Stress-eYFP		q = 6.71, df = 15.94	P = 0.0012	p < 0.01
	Con-eYFP vs. Con-ChR2		q = 0.60, df = 14.84	P = 0.9731	n.s.
	Stress-eYFP vs. Stress-ChR2		q = 1.60, df = 9.78	P = 0.6792	n.s.
	Con-ChR2 vs. Stress-ChR2		q = 11.37, df = 8.66	P = 0.0001	p < 0.001
	ON	Tukey's multiple comparisons test			
	Con-eYFP vs. Stress-eYFP		q = 9.58, df = 11.84	P = 0.0001	p < 0.001
	Con-eYFP vs. Con-ChR2		q = 7.49, df = 11.51	P = 0.0011	p < 0.01
	Stress-eYFP vs. Stress-ChR2		q = 12.92, df = 15.17	P < 0.0001	p < 0.001
	Con-ChR2 vs. Stress-ChR2		q = 7.24, df = 9.92	P = 0.0022	p < 0.01
	OFF	Tukey's multiple comparisons test			
	Con-eYFP vs. Stress-eYFP		q = 6.67, df = 15.54	P = 0.0013	p < 0.01
	Con-eYFP vs. Con-ChR2		q = 0.54, df = 13.33	P = 0.9799	n.s.
D	Stress-eYFP vs. Stress-ChR2		q = 0.61, df = 11.57	P = 0.9716	n.s.
	Con-ChR2 vs. Stress-ChR2		q = 7.27, df = 8.27	P = 0.0036	p < 0.01
	Con-eYFP, Stress: mice = 9,9,9,8	two-way repeated measures ANOVA	group×epoch interaction F (6, 64) = 16.20	p < 0.0001	p < 0.001
	OFF	Tukey's multiple comparisons test			
	Con-eYFP vs. Stress-eYFP		q = 6.09, df = 15.42	P = 0.0030	p < 0.01
	Con-eYFP vs. Con-ChR2		q = 0.33, df = 14.41	P = 0.9951	n.s.

	Stress-eYFP vs. Stress-ChR2		q = 0.52, df = 16.66	P = 0.9824	n.s.
	Con-ChR2 vs. Stress-ChR2		q = 6.53, df = 12.55	P = 0.0026	p < 0.01
	ON	Tukey's multiple comparisons test			
	Con-eYFP vs. Stress-eYFP		q = 6.44, df = 15.65	P = 0.0018	p < 0.01
	Con-eYFP vs. Con-ChR2		q = 6.39, df = 10.59	P = 0.0045	p < 0.01
	Stress-eYFP vs. Stress-ChR2		q = 10.14, df = 13.35	P < 0.0001	p < 0.001
	Con-ChR2 vs. Stress-ChR2		q = 1.31, df = 14.91	P = 0.7933	n.s.
	OFF	Tukey's multiple comparisons test			
	Con-eYFP vs. Stress-eYFP		q = 6.43, df = 15.38	P = 0.0019	p < 0.01
	Con-eYFP vs. Con-ChR2		q = 0.31, df = 14.16	P = 0.9962	n.s.
	Stress-eYFP vs. Stress-ChR2		q = 1.70, df = 16.32	P = 0.6344	n.s.
	Con-ChR2 vs. Stress-ChR2		q = 7.66, df = 15.51	P = 0.0009	p < 0.001
E	Con-eYFP, Stress: mice = 9,9,9,8	two-way repeated measures ANOVA	group×epoch interaction F (6, 64) = 0.1177	P = 0.9940	n.s.

Supplementary figure2						
C	eYFP vs ChR2	mice = 8,8	two-way repeated measures ANOVA	group×epoch interaction F (2, 28) = 3.183	P = 0.0568	n.s.
D	eYFP vs ChR2	mice = 8,8	two-way repeated measures ANOVA	group×epoch interaction F (2, 28) = 4.989	P = 0.0140	p < 0.05
	OFF		Bonferroni's multiple comparisons test	t = 0.18, df = 13.40	p > 0.9999	n.s.
	ON		Bonferroni's multiple comparisons test	t = 3.02, df = 13.69	p = 0.0284	p < 0.05
	OFF		Bonferroni's multiple comparisons test	t = 0.46, df = 13.06	p > 0.9999	n.s.
E	eYFP vs ChR2	mice = 8,8	two-way repeated measures ANOVA	group×epoch interaction F (2, 28) = 5.337	P = 0.0109	p < 0.05
	OFF		Bonferroni's multiple comparisons test	t = 0.33, df = 13.75	p > 0.9999	n.s.
	ON		Bonferroni's multiple comparisons test	t = 3.29, df = 8.86	p = 0.0284	p < 0.05
	OFF		Bonferroni's multiple comparisons test	t = 1.25, df = 13.72	p = 0.6992	n.s.

F	eYFP vs Chr2	mice = 8,8	two-way repeated measures ANOVA	group×epoch interaction F (2, 28) = 0.2526	$P = 0.7785$	<i>n.s.</i>
Supplementary figure 5						
C	eYFP vs Chr2	mice = 8,9	two-way repeated measures ANOVA	group×epoch interaction F (2, 30) = 1.205	$P = 0.3138$	<i>n.s.</i>
D	eYFP vs Chr2	mice = 8,9	two-way repeated measures ANOVA	group×epoch interaction F (2, 30) = 0.4929	$P = 0.6157$	<i>n.s.</i>
E	eYFP vs Chr2	mice = 8,9	two-way repeated measures ANOVA	group×epoch interaction F (2, 30) = 0.7819	$P = 0.4666$	<i>n.s.</i>
F	eYFP vs Chr2	mice = 8,9	two-way repeated measures ANOVA	group×epoch interaction F (2, 30) = 0.3700	$P = 0.6938$	<i>n.s.</i>
I	eYFP vs Chr2	mice = 12,12	two-way repeated measures ANOVA	group×epoch interaction F (2, 44) = 0.05237	$P = 0.9490$	<i>n.s.</i>
J	eYFP vs Chr2	mice = 12,12	two-way repeated measures ANOVA	group×epoch interaction F (2, 44) = 0.4984	$P = 0.6109$	<i>n.s.</i>
K	eYFP vs Chr2	mice = 12,12	two-way repeated measures ANOVA	group×epoch interaction F (2, 44) = 0.1886	$P = 0.8287$	<i>n.s.</i>
L	eYFP vs Chr2	mice = 12,12	two-way repeated measures ANOVA	group×epoch interaction F (2, 44) = 0.3683	$P = 0.6940$	<i>n.s.</i>
Supplementary figure 9						
B	eYFP, Chr2, eNpH	mice = 8,8,8				
	retrial		one-way ANOVA	F (2, 21) = 32.07	$P < 0.0001$	$P < 0.001$
	eYFP vs Chr2		Dunnett's multiple comparisons test	q = 7.273, df = 21	$P < 0.0001$	$P < 0.001$
	eYFP vs eNpHR		Dunnett's multiple comparisons test	q = 0.731, df = 21	$P = 0.6895$	<i>n.s.</i>
	fear extinction		two-way repeated measures ANOVA	group×epoch interaction F (18,189) = 9.718	$P < 0.0001$	$P < 0.0001$
	eYFP vs Chr2		Dunnett's multiple comparisons test	q = 10.04, df = 116.3	$P < 0.0001$	$p < 0.0001$
	eYFP vs eNpHR		Dunnett's multiple comparisons test	q = 0.5728, df = 156.6	$P = 0.7905$	<i>n.s.</i>
	extinction retrial		one-way ANOVA	F (2, 21) = 112.4	$P < 0.0001$	$P < 0.001$
	eYFP vs Chr2		Dunnett's multiple comparisons test	q = 7.79, df = 21	$P < 0.0001$	$p < 0.001$
	eYFP vs eNpHR		Dunnett's multiple comparisons test	q = 7.19, df = 21	$P < 0.0001$	$P < 0.001$
C	eYFP, Chr2, eNpH	mice = 9,9,8				

	retrial		one-way ANOVA	F (2, 23) = 0.05411	$P = 0.9474$	<i>n.s.</i>
	fear extinction		two-way repeated measures ANOVA	F (18, 207) = 0.1637	$P > 0.9999$	<i>n.s.</i>
	extinction retrial		one-way ANOVA	F (2, 23) = 0.2518	$P = 0.7795$	<i>n.s.</i>